FINAL TECHNICAL REPORT

Empirical Relationships between Lithology and Shear Wave Velocity; Revised Digital NEHRP Site Classification Maps for Albuquerque, New Mexico

Recipient:

[1]Fugro William Lettis & Associates, Inc.,
1777 Botelho Dr., Ste. 262, Walnut Creek, CA 94596
(925) 256-6070 phone; (925)256-6076 fax; URL www.lettis.com

Principal Investigators:

Kevin B. Clahan[1], James P. Turner[2], Andrew T. Lutz, Mark S. Zellman
K.Clahan@fugro.com[1], J.Turner@fugro.com[2]

Contributors:

Daniel R.H. O'Connell

Keywords:

Soil Classification, Vs30, Shear wave velocity, New Mexico, Albuquerque, NEHRP, Classification Maps, IMASW, Interferometric Multichannel Analysis of Surface Waves, Ground Motions, Amplification

Program Element I

U. S. Geological Survey
National Earthquake Hazards Reduction Program
Award Number G09AP00129

9/01/09 through 8/31/10

Research supported by the U.S. Geological Survey (USGS), Department of the Interior, under USGS award number G09AP00129. The views and conclusions contained in this document are those of the authors and should not be interpreted as necessarily representing the official policies, either expressed or implied, of the U.S. Government.

Award G09AP00129

Empirical Relationships between Lithology and Shear Wave Velocity; Revised Digital NEHRP Site Classification Maps for Albuquerque, New Mexico

Kevin B. Clahan[1], James P. Turner[2], Andrew T. Lutz, Mark S. Zellman,
[1]Fugro (Hong Kong) Limited, William Lettis & Associates, Inc., 7/F., Guardian House
32 Oi Kwan Road Wanchai, 842, Hong Kong
(852) 2894 5828 phone, k.clahan@fugro.com
[2]Fugro William Lettis & Associates, Inc., 436 Cole Boulevard, Suite 230, Lakewood, CO, 80401
(720) 836-4880 phone, j.turner@fugro.com

ABSTRACT

New site-specific shear wave velocity structure profiles were measured across a representative range of surficial geologic deposits to characterize seismogenic ground shaking hazards in Albuquerque, New Mexico. Albuquerque (population roughly 870,000) is a rapidly developing metropolitan area constructed in large part on young, unconsolidated alluvium in the seismically active Rio Grande rift valley. Albuquerque is located adjacent to the Sandia range-front fault system, which can produce earthquakes as strong as Mw7.0. Interferometric MASW surface shear wave geophysical survey methods were used to calculate 62 high-resolution shallow shear wave velocity profiles in order to develop empirical relationships between shear wave velocity and lithology, and to produce a predictive hazard map of seismically-induced ground shaking in the Middle Rio Grande valley. The results of this analysis show that shear wave velocity structure in the Albuquerque area is generally homogenous, typically characterized by 5 to 10 meters of slow (≤200 m/s) and unconsolidated Holocene alluvium over faster (>400 m/s) and more consolidated Pleistocene alluvium. Shallow, unconsolidated alluvium generally produces strong amplification of ground motions, and the results of this study predict that the strongest amplifications will occur in Holocene fluvial deposits located near downtown and in a north-south corridor along the active Rio Grande channel and floodplain. Strong amplifications are expected to occur in the 2 to 3 Hz bandwidth window, resonance frequencies that correspond closely to natural response frequencies of two to four story buildings. These zones of expected strong amplification are well defined by 5 meter depth-averaged shear wave velocity NEHRP classification mapping. This study demonstrates that cost efficient site-specific velocity structure surveys can significantly improve the delineation of shallow strong ground motion amplification zones where impacts to building performance and emergency response are expected to be most severe during an earthquake. Additionally, these data also provide high quality design inputs for future construction of engineered structures.

TABLE OF CONTENTS

ABSTRACT I
1.0 INTRODUCTION 1
1.1 Geologic Setting 1
1.2 Integration with Existing Work 2
2.0 SHEAR-WAVE VELOCITY SURVEYS 3
2.1 Field Methodology 3
2.2 Interferometric MASW 4
2.3 Vs Data Processing 5
3.0 CLASSIFICATION METHODOLOGY 6
3.1 Composite Shear-wave Velocity Profiles 6
3.2 Relation of Vs profiles to geologic units based on surficial geology 7
3.3 Defining Vs-Lithologic Units: Correlating Velocity Structure to Surficial Geologic Units 7
3.3.1 Unit Qrpx, Rio Grande River channel and fluvial terrace deposits (Holocene) 8
3.3.2 Unit Qrx, Rio Grande River fluvial terrace deposits (Pleistocene) 9
3.3.3 Unit Qax, Stream valley alluvium (Latest Pleistocene to Holocene) 9
3.3.4 Unit QTsx, Fluvial and piedmont deposits (Pliocene to lower Pleistocene) 9
3.3.5 Unit Tcrg, Older alluvium (Pliocene to lower Pleistocene) 9
3.3.6 Unit Qam, Intermediate stream valley alluvium (Pleistocene to Holocene) 10
3.3.7 Unit Qao, Older stream-valley alluvium (middle Pleistocene) 11
3.3.8 Unit Qb, Basalt (Middle Pleistocene) 11
4.0 RESULTS 12
4.1 Predictive site response NEHRP classification maps (1:24,000-scale) 12
4.2 Comparison of IMASW Vs30 maps to USGS Map Server and Distance-from-bedrock maps 12
4.3 Shallow Amplification Effects 12
5.0 CONCLUSIONS 14
6.0 ACKNOWLEDGEMENTS 15
7.0 REFERENCES 16

8.0 APPENDICES 19

LIST OF TABLES

Table 1. NEHRP Soil Classification with Wills et al. (2000) modified subclasses..... 7

Table 2. Vs-Lithologic Classification summary from 62 site-specific IMASW survey profiles . 10

LIST OF FIGURES

Figure 1. Location Map
Figure 2. IMASW Survey Locations and Geologic Map
Figure 3. Composite Vs-Structure Plots
Figure 4. Vs-lithologic Units
Figure 5. Vs2, Vs5, Vs10, and Vs15 Classification Maps
Figure 6. Vs20, Vs25, Vs30, and Vs50 Classification Maps
Figure 7. Comparison: IMASW Vs30 vs. USGS Map Server Vs30
Figure 8. Shallow Amplification Factors

LIST OF APPENDICES

Appendix A. IMASW Shear Wave Velocity Profiles
Appendix B. NCF Waveform and slowness-frequency Picks.

1.0 INTRODUCTION

This study develops empirical relationships between subsurface shear wave velocity (Vs) and lithologic properties of surficial geologic units in order to produce a predictive microzonation map of expected shallow surficial response to strong ground motions. Similar empirical relationships between surficial geology and subsurface shear wave velocity have been used for many years to predict ground motion amplification (e.g., Joyner and Fumal, 1985; Boore et al., 1993; Borcherdt, 1994; Holzer et al., 2002; 2005), and shear wave velocity is a well-accepted and widely used measure of rock or soil conditions for calculating ground motions for soil and rock (e.g., Fumal, 1978; Fumal and Tinsley, 1985; Park and Elrick, 1998). Geologic units were correlated into groups that are expected to perform similarly based on the Vs-based NEHRP soil classification criteria. This method has been applied in other recent studies at local (e.g., Scott et al., 2006), regional (e.g., Wills and Clahan, 2006; Louie, 2008), and national (e.g., Petersen et al., 2008) scales. In addition to the NEHERP classification maps, results of this study provide quantitative Vs inputs for future site classification efforts, NGA ground shaking modeling efforts, and calculations of expected amplification factors for the Albuquerque metropolitan area.

Sixty-two sites were surveyed in June 2010 using the recently developed Interferometric Multichannel Analysis of Surface Waves (IMASW) method (O'Connell and Turner, submitted, reviewed) to measure shear wave velocities across a representative range of geologic units. The IMASW method was designed to measure site-specific line-averaged shear wave velocity profiles to a minimum depth of 30 meters (Vs30), though IMASW surveys can resolve shear wave velocity structure significantly deeper than 30 meters. The resulting line-averaged shear wave velocity values were calculated for a variety of depths from 2 to 100 meters (Vs2 to Vs100), and these values were compiled to develop a characteristic Vs model for each major surficial geologic unit mapped by Connell (2006). The geologic units defined by Connell (2006) were subsequently grouped by similar Vs characteristics to develop a set of Vs-lithologic units used here to examine the relationships between lithology and shear wave velocity.

The primary geologic units included in this approach were differentiated by Connell (2006) in terms of variation in age, depositional process, and grain size. For each Vs-lithologic unit, composite log-mean Vs profiles were calculated to produce revised predictive site-response maps for Albuquerque, New Mexico. Additionally, amplification factors were calculated for Vs-lithologic units to predict areas expected to experience increased ground motions during strong ground shaking (Boore, 2003).

1.1 Geologic Setting

Albuquerque is located in the seismically active Rio Grande rift valley (Figure 1), where previous studies have determined that the Sandia-Rincon fault along the western margin of the Sandia Mountains can produce large surface-rupturing earthquakes (Mw 7.0) (Kelson et al., 1999; Personius et al., 2001). Additional recognized seismic sources in the Albuquerque area include the West Mesa fault zone (west of the Rio Grande), and the Hubbell Springs fault (bordering the Manzanita and Manzano Mountains) (Machette et al., 1998; 2004; Wong et al.,

2004; Connell, 2006). Uplifted Proterozoic granite in the Sandia Mountains bounds the Rio Grande Rift to the east, and active north-striking normal faults in the rift valley have produced roughly 3,300 meters of west-down vertical separation across a 30-km-wide zone between the Rio Grande river and the Sandia peaks (Connell, 2006). Paleoseismic studies suggest that large earthquakes were produced along this system in the late Holocene (Machette et al., 1998; Personius et al., 1999; 2001; Machette, 2008; McCalpin, 2008; Zachariasen and Olig, 2008), and these faults are considered to be capable of generating ground motions on the order of 0.3 g to 0.6 g peak ground acceleration (1 g = 980 cm/sec^2) for the 500- and 2,500-yr return periods, respectively (Wong et al., 2004). The predicted ground motions are possibly strong enough to trigger liquefaction in unconsolidated river and floodplain sediments (Kelson et al., 1999; Hitchcock and Kelson, 2007). The Rio Grande rift valley is underlain by Proterozoic to Cenozoic basement rock and partly consolidated Neogene to Holocene basin deposits of varying thicknesses with sufficient variation in grain size, induration, and thickness to produce variable responses to strong ground motions.

1.2 Integration with Existing Work

This research builds on existing NEHRP-funded projects performed by Fugro WLA geologists in the Albuquerque area, including liquefaction susceptibility mapping (Kelson et al., 1999) and liquefaction and permanent surface deformation mapping (Hitchcock and Kelson, 2007). The products of this study incorporate existing geologic mapping and digital map products for the Albuquerque-Rio Rancho Metropolitan Area and Vicinity (Connell, 2006; Williams and Cole, 2007) to develop predictive site-response maps in a GIS database. This study applies the Vs-lithologic classification methods developed by Wills and Clahan (2006) and Wills and Gutierrez (2008) and compares the high-resolution IMASW-based classification results (O'Connell and Turner, submitted, revised) to the widely used USGS Vs30 MapServer remote sensing method (Wald and Allen, 2007) that uses topographic slope as a regional proxy for Vs30 in tectonically active regions. This study also compliments existing efforts to collect and analyze site conditions using non-intrusive surface wave analysis (Holzer, et al., 2002; 2005; Scott et al., 2004; 2006; Stephenson et al., 2005; Thelen et al., 2006) and provide data to update ongoing national mapping of probabilistic seismic hazard (Wong et al., 2004, Petersen et al., 2008).

2.0 SHEAR WAVE VELOCITY SURVEYS

The IMASW shear wave velocity surveys were collected in June 2010 on publicly-owned properties managed by the City of Albuquerque Department Parks and Recreation and the Albuquerque Open Space Program (Figure 2). The IMASW survey locations and azimuthal orientations of the geophone arrays were planned to satisfy several conditions. Most importantly, survey locations were aligned to measure representative velocity structure for targeted surficial geologic units across a representative range of geographic locations. Because the IMASW results provide a vertical shear wave velocity profile averaged horizontally over the length of the line, the position of each survey was designed to measure velocity structure within a single surficial geologic unit and to avoid crossing geologic contacts. Additionally, the IMASW lines were generally oriented perpendicular to directed background noise sources (railways, construction sites, highways) to maximize seismic wave propagation parallel to the geophone sensor array, and to avoid broad-siding the array with noise for optimal fundamental mode illumination in the 2 to 60 Hz bandwidth window.

Eighty shear wave velocity surveys were proposed prior to the start of field data collection, based on a desktop reconnaissance of the targeted geologic units. This study was limited to 62 useful IMASW shear wave velocity surveys, primarily due to the limited aerial extent of targeted geologic units on publicly accessible land, as well as poor data quality in certain locations due to poor geophone coupling and seismic source attenuation on proposed locations where eolian sand is thicker than 2 m. The Vs-depth profiles calculated for the 62 IMASW surveys are provided in Appendix A.

2.1 Field Methodology

The IMASW data were collected using a DAQLink II 24-bit Acquisition System unit, twelve 4.5Hz vertical-component geophones, an 88 m seismic array cable with 8 m geophone spacing, and a Panasonic Toughbook computer with VScope version 2.4.20 and IMASW version 1.1 software. This equipment was calibration tested and verified to operate properly at the Applied Technical Services ISO 17025 (A2LA) accredited calibration testing facility in Marietta, Georgia, on June 24, 2009.

Interferometric processing methods require records of active-source noise produced at various distances off both ends of each survey line. To supplement background noise and ensure acquisition of good quality high frequency (> 5 Hz) data, active noise was produced using a 1-inch-thick steel strike plate and an 11.5 lb Stanley composite dead-blow sledgehammer (designed to prevent rebounding and couple more energy to the ground compared to a steel hammer). Where possible, the IMASW surveys were located perpendicular to nearby indigenous seismic energy sources (e.g., overpass foundations and roadways) to exploit ambient low-frequency fundamental mode excitation at frequencies below 8 Hz and illuminate deeper velocity structure (>30 meters) (O'Connell, 2007). In comparison, active noise sources (such as hammer and strike plate) used alone cannot excite fundamental modes below about 8 Hz. Data acquisition at each survey location began with geophone testing to ensure adequate coupling with the ground

surface and proper connection to the data cable. Active and background noise sources were recorded in 20 to 40 minute intervals for each IMASW survey line. Slowness-frequency (p-f) images were calculated for each IMASW site survey during data acquisition and were evaluated on-site to ensure that sufficient data were recorded. If higher modes or broadside noise pollution were determined to be dominating the signal, the geophone array or active seismic source were reconfigured until quality fundamental mode p-f dispersion curves were achieved.

2.2 Interferometric MASW

Refraction microtremor (ReMi) and multichannel analysis of surface waves (MASW) are two effective approaches to estimate shallow shear wave velocity structure. This study used the IMASW method, a recently developed data acquisition and interferometric processing approach (Curtis et al. 2006; Bensen et al., 2007; Snieder et al, 2009) that combines the active source data acquisition typical of MASW (Park et al., 1999) and the ambient noise typically recorded in ReMi data (Louie, 2001) in order to improve Vs-depth resolution and increase the maximum depth of significant Vs resolution. The IMASW method improves resolution of low frequency phase and group velocities relative to p-f, increases the maximum depth resolution of shear wave velocities relative to MASW and ReMi, and provides data uncertainty constraints that indicate maximum depth of shear wave velocity resolution. The primary objectives of IMASW investigations are to model vertical variation in shallow shear wave velocity structure within the dimensions of each individual survey line and to estimate 30 m depth-averaged shear wave velocities (Vs30) along each survey alignment. In some ideal circumstances IMASW surveys received sufficient low frequency surface wave signals to estimate shear wave velocities to 200 m depth. Sufficient data were obtained during this study to calculate shear wave velocities to 30 m for all IMASW line profiles, and shallow velocity structure is well constrained at depths <30 m. Typical frequency bandwidth of well resolved phase velocities varies over the frequency range of 2 Hz to 60 Hz, with most IMASW lines obtaining good resolution of phase and group velocities in the 4 Hz to 35 Hz frequency band. Noise correlation function (NCF) based phase and group velocity waveform picks provide additional phase- and group-velocity constraints that enhance p-f image picking by improving low frequency (<10 Hz) data resolution where p-f images typically lose resolution. NCF phase- and group-velocity picks and p-f picks are included in Appendix B.

As described above, the technique used in this study combined p-f slant-stack analyses with time-domain dispersion analyses using seismic interferometry to estimate Rayleigh-wave dispersion. Cross-correlation interferometry is used to obtain deterministic correlation Green's function (CGF) IMASW seismograms from ambient noise and/or active-source wavefields contained in ReMi and/or MASW data. The CGFs were processed using the multiple filter technique to estimate phase and group dispersion. Using the IMASW method, active seismic sources ensure that the stationary phase contributions to cross-correlations dominate CGF responses. In a single IMASW profile, each geophone represents a virtual source. The IMASW method stacks CGF common offset data from all virtual sources to obtain a single averaged forward and reverse record section. CGF-time-domain and p-f phase slowness estimates are combined with CGF-time-domain group slowness estimates to provide a consistency check for dispersion picks, improving resolution of velocity variations with depth and increasing the

maximum depth of significant velocity resolution. A multi-state Monte Carlo approach is used to estimate mean slowness-depth and slowness uncertainties.

The IMASW processing and slowness-depth inversion approach has been evaluated using passive ReMi data from two sites and active-source IMASW at six sites with independent velocity-depth logs. Comparison of six P-S suspension log-IMASW profile pairs across the Van Norman Complex in northern San Fernando Valley shows that on average 30-m-depth shear wave velocity (Vs30) estimates between the two methods differed by <1% (O'Connell and Turner, submitted, revised).

2.3 Shear Wave Data Processing

Data were exported in .SEGY format using Seismic Source Company's Vscope software and were read into IMASW v. 1.1 software and processed separately as forward stacks (geophone 1 to 12) and reverse stacks (geophone 12 to 1). Undesirable higher mode dominated or polluted noise records were removed from the final forward and reverse stacks to make the cleanest possible fundamental mode Rayleigh wave dispersion curves for each processing direction. Forward- and reverse-stacked dispersion curves were stacked together to make line averaged combined dispersion curves. NCF group- and phase-velocity processing constrains fundamental mode p-f picks, and the p-f uncertainty picks were made on the best combined fundamental-mode p-f dispersion curve for each survey. Subsequently the p-f picks were inverted using a 5-batch iterative Monte Carlo approach that evaluates approximately 14,000 models, yields final inversion output parameters, and runs a final inversion evaluating 4000 to 10,000 models to calculate the final most statistically feasible Vs structure. Shallow shear wave velocity structure results are based on best-fit models of Rayleigh wave dispersion curves. Resulting Vs-depth profiles (Appendix A) show the interpreted shear wave velocity structure for each of the 62 IMASW survey lines. Table 2 contains tabulated Vs-depth data organized by surficial geologic unit. The 62 IMASW Rayleigh wave phase-p-f images with p-f picks are included in Appendix B.

3.0 CLASSIFICATION METHODOLOGY

Consistent methods have been developed for characterizing shear wave structure using empirical relationships between surficial geology and subsurface shear wave velocity to estimate ground motion amplification predictions (e.g., Joyner and Fumal, 1985; Boore et al., 1993; Borcherdt, 1994; Holzer et al., 2002; 2005). This section describes the methods used to correlate geologic units combining high resolution site-specific IMASW surface survey data, existing geologic maps (Connell, 2006), and NEHRP soil classification criteria (Table 1). A similar method has been performed at local (e.g., Scott et al., 2006) and regional (e.g., Wills and Clahan, 2006; Louie, 2008) scales by compiling existing Vs30 data and extrapolating velocity structure to similar geologic deposits. The IMASW site-specific surveys performed for this study provide high-resolution constraints on shallow velocity structure (2 to 30 meters) that provide an increased level of understanding for ground shaking and amplification parameters in the Albuquerque using similar classification methodology.

Several additional considerations must be made when classifying ground shaking behavior of surficial geologic deposits using Vs30 values. First, many of the young unconsolidated alluvial units are less than 30 meters thick in the Albuquerque region. For example, the inner Rio Grande valley in Albuquerque includes several unconsolidated surficial units, typically about 2 to 10 meters thick, including relatively slow alluvium (≤200 m/s) that overlies older, faster (>400 m/s) deposits, a condition that is expected to amplify ground motions. These older-faster deposits project under the inner valley from the east and west and include the Pliocene-Pleistocene Ceja Formation (Tcrg) and the Miocene to Pleistocene Sierra Ladrones Formation (QTs). Results from the high-resolution IMASW surveys in this study indicate that Vs estimates in 5 meter increments to depths of 30 meters do adequately resolve the slower unconsolidated alluvial materials that are of primary concern in estimating ground shaking hazards, demonstrating the importance of using the data in a way that reveals the resolution of the shallow velocity structure measured by IMASW surveys.

3.1 Composite Shear Wave Velocity Profiles

Figure 3 shows composite Vs-depth profiles classified by surficial geologic unit. The criteria for aggregating the highly detailed map units of Connell (2006) into generalized Vs-geologic classes are discussed below in Section 3.3 (Figure 4). A significant trend depicted in the composite profiles (other than those in high-velocity basalt) is the previously described condition where roughly 5 to 10 meters of slow (≤200 m/s/) deposits overlie a thicker section of faster (>400 m/s) Vs structure. This pattern is recognized across the Rio Grande valley, indicating that the distribution of shallow surficial deposits and velocity structure is remarkably consistent (Figure 3).

Depth-Vs values calculated for each IMASW survey profile are tabulated in Table 2, which includes depth-averaged shear wave velocity values calculated for depth intervals at 2, 5, 10, 15, 20, 25, 30, 50, and 100 meters (Figures 5 and 6).

3.2 Relation of Vs profiles to geologic units based on surficial geology

Maps of geologic units that can be distinguished by their shear wave velocities at various depth levels were developed for this study using the methods described by Wills and Clahan (2006) (Figures 5 and 6). Statistical analyses of Vs structure yield mean and standard deviation Vs values, and the mean Vs value was then classified according to the NEHRP soil classification scheme and adjusted using Wald and Allen's (2007) modified subclasses (e.g. D1, D2, D3) for site-specific Vs (Table 1) (FEMA, 1994; Wills et al., 2000; Wald and Allen, 2007).

Class		Vs30 Range (m/sec)
E		< 180
D	D1	180 - 240
	D2	240 - 300
	D3	300 - 360
C	C1	360 - 490
	C2	490 - 620
	C3	620 - 760
B		> 760

Table 1. NEHRP Soil Classification with Wills et al. (2000) modified subclasses

3.3 Defining Vs-Lithologic Units: Correlating Velocity Structure to Surficial Geology

The composite Vs-depth profiles (Figure 3) define the basis for applying characteristic shear wave velocities directly to detailed geologic units mapped and described in four 7.5-minute quadrangles (Los Griegos, Alameda, Albuquerque West, and Albuquerque East) in the study area (Connell, 2006). Figure 4 shows the aggregated Vs-lithologic unit classification map created by combining existing detailed map units (Connell, 2006) into more generalized map units defined by empirical relationships between surficial geology and characteristic shear wave velocity. Unit symbols ending in "x" indicate that multiple geologic map units have been combined into generalized Vs-lithologic units defined by Vs-lithologic relationships. For example, geologic map units Qa and Qay were combined to form the Vs-lithologic unit Qax to indicate their similar genetic depositional processes and characteristic velocity structure.

Log-mean averaged Vs-depth profiles were calculated for each Vs-lithologic unit from each composite Vs-depth profile (Figure 3). The Vs-depth classification scheme is applied to 1:24,000-scale maps for a suite of depth intervals across the study area. Table 2 summarizes the shear wave velocity characteristics that define the Vs-lithologic map units. Discussion of the mean and standard deviation distribution of Vs30 are included for each unit along with summaries discussing the classification approach used to aggregate the geologic map units of Connell (2006) into aggregated Vs-lithologic units.

There are several caveats when using surficial geology to characterize subsurface velocity structure. For one, the thin nature of some low velocity, unconsolidated surficial eolian sand units in four survey Vs profiles (Lines 48, 52, 61, 62) were too thin (1 to 2 m) to accurately resolve. This is due to the inability of 8 meter geophone spacing to accurately resolve 2- to 3-m-

thick low-velocity zones, and because the unconsolidated sands yield poor geophone coupling and strongly attenuate active seismic source noise. In these cases the Vs profiles have been reassigned to the appropriate underlying geologic unit. Line 48 was reassigned to unit Tcrg, Line 52 to unit QTsx, and Lines 61 and 62 to unit Qb (Table 2, Appendix A).

Composite Vs plots (Figure 3) show 88 m array line-averaged Vs-depth structure for each IMASW survey location. Other than IMASW surveys directly measured on units Tcrg or QTxs, each profile is measuring the velocity structure of various surficial units overlying relatively faster unit Tcrg or QTsx at depth. Based on line-averaged composite velocity plots, the depth to this velocity increase is generally 5 to 10 meters. Because the primary focus of this microzonation study is to accurately delineate soils prone to the strongest ground shaking and amplification, it is important to assess velocity structure at depth increments shallower than Vs30 (<30 m).

NEHRP soil classification criteria (FEMA, 1994) provide a useful scheme to classify ground shaking hazards using shear wave velocity; NEHRP soil classes are applied across a range of Vs-depth values to delineate soils prone to the strongest ground shaking and amplification. To accurately delineate zones most prone to destructive ground shaking, it is necessary to assess the shallower velocity structure in Albuquerque where most unconsolidated surficial units are less than 10 meters thick. Ground motion amplification calculations (discussed in detail in Section 4.3) confirm the usefulness of using 5 meter depth-averaged shear wave velocity (Vs5) to apply NEHRP soil classification criteria (FEMA, 1994) for some surficial geologic units in the Albuquerque area. Vs5 values calculated from IMASW survey profiles were used to delineate the Vs-lithologic units with highest predicted ground shaking hazards. The Vs-lithologic units in the following text are arranged in descending order from slowest to fastest 5 meter depth-averaged shear wave velocity (Vs5).

3.3.1 Unit Qrpx, Rio Grande River channel and fluvial terrace deposits (Holocene)

Ten IMASW survey profiles were measured and calculated for Holocene Rio Grande channel and fluvial terrace deposits (unit Qrpx). Unit Qrpx include clays, silts, sands, and gravels of the active channel and active floodplain deposits adjacent to the Rio Grande River. Connell (2006) identified eight subunits within the Rio Grande River channel and fluvial terraces. These units were all combined into unit Qrpx based on homogenous shear wave velocity structure, similar genetic depositional processes, and similar age. Unit Qrpx deposits are inset into the relatively faster Pliocene-Pleistocene Ceja Formation (Tcrg; Connell, 2006). The mean Vs30 value of unit Qrpx is 379 m/s, however, the Vs profiles indicate that unit Qrpx is approximately 7 to 10 meters thick at all surveyed locations. Because of this, a more appropriate measure of shear wave response is the Vs5 value, which at 159 m/s (NEHRP Soil Class E) represents the highest liquefaction and ground shaking hazard in the study area. Unit Qrpx also has the highest calculated ground shaking amplification in the study area (discussed below in detail in Section 4.3).

3.3.2 Unit Qrx, Rio Grande River fluvial terrace deposits (Pleistocene)

Six IMASW survey profiles were measured and calculated for terrace deposits of the Pleistocene Los Duranes Formation (unit Qrd), present west of the Rio Grande River near West Bluff. No direct measurements were made on the Pleistocene Arenal Formation (unit Qra). However, because unit Qra is lithologically similar to other Pleistocene deposits inset into Qrd, the units Qra and Qrd were combined into the Vs-lithologic unit Qrx. The mean Vs30 value for unit Qrx is 315 m/s, and the mean Vs5 value is 207 m/s (NEHRP Soil Class D1). Unit Qrx has the second highest calculated ground shaking amplification in the study area (Section 4.3).

3.3.3 Unit Qax, Stream valley alluvium (Latest Pleistocene to Holocene)

Sixteen IMASW survey profiles were measured and calculated for unit Qax. Unit Qax includes Quaternary alluvium (unit Qa) and younger stream-valley alluvium (unit Qay) of Connell (2006), both have similar lithologic and shear wave velocity characteristics, and both overlie Pleistocene units Tcrg and QTsx. Unit Qa deposits are located along the flanks of the Rio Grande River terrace deposits, and unit Qay deposits are located in east-west trending arroyos that debouche onto Rio Grande River terrace deposits. Grain size in unit Qax generally fines to the west away from the Sandia range front. The composite profile (Figure 3) for Qax indicates that the unit thickness varies from 2 to 10 meters. The mean Vs30 value for unit Qax is 393 m/s, and the mean Vs5 value is 222 m/s (NEHRP Soil Class D1).

3.3.4 Unit QTsx, Fluvial and piedmont deposits (Pliocene to lower Pleistocene)

Four IMASW survey profiles were measured directly on unit QTsx where it is exposed at the ground surface, and one additional IMASW survey profile (Line 52) was measured in a location where unit QTsx is overlain by 1 to 2m of eolian sand. Line 52 is included with unit QTsx because the IMASW technique could not resolve the Vs structure of the thin, shallow sand. Unit QTsx includes fluvial deposits (unit QTsa) and piedmont deposits (unit QTsp) of the Pleistocene Sierra Ladrones Formation, combined here because of similar age, grain-size, and shear wave velocity characteristics. Though only five direct surveys were measured for unit QTsx, most IMASW survey profiles located east of the Rio Grande River floodplain do measure unit QTsx at various depths, typically 5 to 10 meters below ground surface. Calculated from the five direct IMASW survey profiles, the mean Vs30 value for unit QTsx is 403 m/s, and the mean Vs5 value is 227 (NEHRP Soil Class D1).

3.3.5 Unit Tcrg, Older alluvium (Pliocene to lower Pleistocene)

Two IMASW survey profiles were measured directly on older alluvium unit Tcrg where it is exposed at the ground surface. One additional IMASW survey profile (Line 48) was measured in a location where unit Tcrg is overlain by a thin eolian sand sheet (roughly 1 meter thick). Unit Tcrg was measured at depth in IMASW survey profiles west of the Rio Grande floodplain at 5 to 10 meters depth. Calculated from the three direct IMASW survey profiles, the mean Vs30 value for unit Tcrg is 429 m/s, and the mean Vs5 value is 261 m/s (NEHRP Soil Class D2).

3.3.6 Unit Qam, Intermediate stream valley alluvium (Pleistocene to Holocene)

Thirteen IMASW survey profiles were measured and calculated for intermediate steam valley deposits (unit Qam). Unit Qam is widely distributed across the Albuquerque metropolitan area, and most of the urban residential developments are constructed on unit Qam. Unit Qam includes the interfluves and alluvial fans between the Sandia Mountains and the Rio Grande River and varies from 5 to 43 meters thick. The mean Vs30 value for unit Qam is 412 m/s, and the mean Vs5 value is 236 m/s (NEHRP Soil Class D1).

Vs Unit	Surface Map Unit	Underlying Unit	Vs-depth (m/sec)								
			Vs2	Vs5	Vs10	Vs15	Vs20	Vs25	Vs30	Vs50	Vs100
Qax	Qa	Tcrg	182	222	282	316	340	364	393	487	625
	Qay										
Qam	Qam	QTsx	190	236	291	324	348	374	412	522	728
	Qamt										
Qao	Qao	QTsx	229	265	330	361	391	411	437	544	725
	Qaot										
Qrpx	Qrp	Tcrg	141	159	199	253	304	341	379	520	624
Qrx	Qra	Tcrg	190	207	226	248	270	292	315	424	593
	Qrd										
	Qrm										
	Qre										
	Qrl										
QTsx	QTsa	---	184	227	282	321	345	363	403	510	635
	QTsp										
	Qae	QTsx									
Tcrg	Tcrg	---	182	261	326	361	383	395	429	533	724
	Qe	Tcrg									
Qb	Qb	Tcrg	522	581	606	526	507	539	548	599	843

Table 2. Vs-Lithologic Classification summary from 62 site-specific IMASW survey profiles

The reported value for VsX represents the depth-averaged shear wave velocity at X meters depth. The Vs values increase with depth in all lithologies except Quaternary basalt (unit Qb), which is less than 15 m thick (Connell, 2006). Figure 4 shows the aerial distribution of Vs-lithologic grouped geologic units, and figures 5 and 6 show Vs-lithologic microzonation maps developed from this data.

3.3.7 Unit Qao, Older stream-valley alluvium (middle Pleistocene)

Four IMASW survey profiles were measured and calculated for older stream-valley alluvium (unit Qao) and two profiles for older stream-valley alluvium (unit Qaot1) in Tijeras Canyon are combined with survey profiles in unit Qao, exposed in the southwest portion of the study area near Kirtland. The mean Vs30 value for unit Qao is 437 m/s, and the meanVs5 value is 265 m/s (NEHRP Soil Class D2).

3.3.8 Unit Qb, Basalt (Middle Pleistocene)

Five IMASW survey profiles were measured and calculated for basalt (unit Qb) in the northwest portion of Albuquerque, an area where recent suburban development has been widespread. Five separate basalt flows (units Qb1 to Qb5) mapped by Connell (2006) have been combined here into a single Vs30 classification unit. Unit Qb is typically less than 15 meters thick and forms a high-velocity lid over relatively slower unit Qao deposits, resulting in a mean Vs10 value (606 m/s) that is higher than the mean Vs30 value (548 m/s). The mean Vs5 value is 581 m/s (NEHRP Soil Class C2).

4.0 RESULTS

4.1 Predictive site response NEHRP classification maps (1:24,000-scale)

Figures 5 and 6 contain a suite of Vs-depth-geologic developed from the IMASW survey profiles and subsequent Vs-lithologic classifications. This suite of Vs-depth maps reveal the aerial distribution of velocity structure in the middle Rio Grande valley at depth intervals of 2, 5, 10, 15, 20, 25, 30, and 50 meters, respectively.

4.2 Comparison of IMASW Vs30 Maps to USGS Map Server and Distance-from-bedrock Maps

Figure 7 shows a side-by-side comparison of our site-specific IMASW-derived Vs30 classification map and a map generated using the USGS Vs30 Map Server (Wald and Allen, 2007). The Map Server data use first-order relationships between topographic slope and shear wave velocity to estimate regional Vs30. The USGS Map Server Vs30 map is designed to provide reasonable estimates of regional Vs30, but does not agree well with our site-specific IMASW-based Vs30 map. This could be explained by differences in basin geometry between the Middle Rio Grande valley (thin veneers of young sediment over older deposits) and areas where the models were calibrated (deeper young sediment in the Los Angeles Basin). For the ongoing work on the global USGS Map Server, future investigators could asses a model correction appropriate for continental rift valleys.

4.3 Shallow Amplification Effects

Linear amplifications were calculated for each log-mean composite Vs-profile (Figure 3) from 65 m depth to estimate shallow amplification effects and the resulting impacts on buildings (Figure 8) (Boore, 2003). Ground motions resonating in tune with the natural bandwidth frequencies of buildings cause the most shaking and damage. Building height natural frequencies typically resonate at 10 Hz for single story structures, 5 Hz for two story structures, and 2 Hz for five story structures (MCEER, 2010).

Figure 8a shows that unit Qrpx (Holocene Rio Grande channel and fluvial terrace deposits within 7 meters of the surface) has potential to amplify ground motions by a factor of 3 in the 2 to 3 Hz bandwidth window, the fundamental resonant building frequencies of two to four story structures. Factor 3 is the highest ground shaking amplification hazard in the study area, and locally could significantly amplify peak ground accelerations during seismogenic ground shaking. Unit Qrpx corresponds to the NEHRP Soil Class E red-zone in the Vs2 and Vs5 maps (Figures 5a and 5b), including much of downtown Albuquerque where older two to four story brick buildings are common and could sustain significant damage if founded in this unit.

Linear amplification profiles can be further simplified by grouping surficial Vs-lithologic classes that exhibit similar amplification behaviors (Figure 8b). Units QTsx, Qa, and Qam display similar bimodal amplification peaks at an amplification factor of 2.2 in the 2 to 3 Hz bandwidth

window and peak at a factor of 2.2 at 10 Hz, the fundamental resonant building frequency for single story structures. Units Qao and Qay amplify by a factor of 1.9 in the 3 to 4 Hz bandwidth window, and peak at a factor of 2.2 in the 10 to 20 Hz bandwidth window at the fundamental resonant building frequency for single story structures. As expected, unit Qb (Quaternary basalt) bedrock does not significantly amplify ground motions. Unit Qrx amplification peaks at a factor of 2.2 in the 2 to 3 Hz bandwidth window at the natural frequencies of four to five story structures.

5.0 CONCLUSIONS

The City of Albuquerque, New Mexico (population roughly 870,000) is located adjacent to the seismically active Sandia range-front fault system, capable of Mw 7.0 earthquakes, and significant portions of the city are developed on young, unconsolidated alluvium. Site-specific, high-resolution shear wave velocity was measured using the Interferometric MASW method at 62 sites across a representative range of surficial geologic deposits in Albuquerque to develop empirical relationships between shear wave velocity and lithology. Empirical Vs-lithologic relationships developed lithology-based predictions of seismically-induced ground shaking hazards in the Middle Rio Grande valley.

The shallow soil conditions in Albuquerque are characterized by a relatively homogenous soil velocity profile, with roughly 5 to 10 meters of slow (≤200 m/s) unconsolidated alluvium over fast (>400 m/s) older alluvium that results in as few as 5 characteristic frequency-amplification responses. This pattern is recognized in nearly all measured locations across the Rio Grande valley as part of this study. The strongest amplifications are expected to occur in Holocene Rio Grande River channel and fluvial terrace deposits (Unit Qrpx) in the downtown area and along a north-south corridor in the active channel and floodplain. Unit Qrpx deposits are typically 7 meters thick, unconsolidated, NEHRP Soil Class E (Vs ≤ 180 m/s) fluvium that overly more consolidated Pliocene-Pleistocene Ceja Formation. Unit Qrpx is characterized by velocity structure predicted to amplify ground motion by a factor of 3 with natural resonant frequencies that are expected to cause severe damage to two to four story buildings founded in this unit. Unit Qrpx fluvial deposits represents the highest ground shaking and liquefaction hazard in the study area. However, all alluvial units (Qrx, Qax, QTsx, Tcrg, Qam, and Qao) in the study area are classified as NEHRP Class D soils at 5 meters depth, and are expected to amplify ground motions by at least a factor of 2. Therefore, a 0.3 g ground motion emanating from the Sandia-Rincon fault at depth could potentially amplify shallow peak ground accelerations by a factor of 2 to 3, which could locally generate peak ground accelerations of 0.6 g and 0.9 g.

6.0 ACKNOWLEDGEMENTS

We would like to thank George Schroder of the Bernalillo County Department of Environmental Health for providing guidance and logistical assistance in obtaining permits to perform this work, the City of Albuquerque Department of Parks and Recreation and Open Space Division for permission to perform this study on public lands, Sean Connell for his invaluable detailed mapping and geologic descriptions, Ivan Wong for providing materials from previous ground motion studies in the area, Keith Kelson for guidance and for discussions about his studies of liquefaction potential in Albuquerque, and Dan O'Connell for important project support and discussions about his IMASW software.

7.0 REFERENCES

Boore, D.M., 2003, 85.13 SMSIM: Stochastic Method SIMulation of Ground Motion from Earthquakes, International Handbook of Earthquake Engineering Seismology, v. 81B, p. 1631-1632.

Boore, D.M., Joyner, W.B., and Fumal, T.E., 1993, Estimation of response spectra and peak accelerations from western North American earthquakes: an interim report, U.S. Geological Survey Open-File Report 93-509, 72 p.

Borcherdt, R.D., 1994, Estimates of site-dependent response spectra for design (methodology and justification): Earthquake Spectra, v. 10, p. 617-654.

Connell, S.D., 2006, Preliminary geologic map of the Albuquerque-Rio Rancho metropolitan area and vicinity, Bernalillo and Sandoval Counties, New Mexico: New Mexico Bureau of Mines and Mineral Resources, Open-File Report 496, version 2.0, scale 1:50,000.

FEMA 222A (1994), NEHRP recommended provisions for the development of seismic regulations for new buildings, 1994 edition, Part 1 – provisions, Federal Emergency Management Agency, 290 pp.

Fumal, T.E., 1978, Correlations between seismic wave velocities and physical properties of near-surface geologic materials in the southern San Francisco Bay region, California: U.S. Geological Survey Open-File Report 78-1067.

Fumal, T.E., and Tinsley, J.C., 1985, Mapping shear wave velocities in near-surface geologic materials, in Ziony, J.I. (ed.), Evaluating Earthquake Hazards in the Los Angeles Region: An Earth Science Perspective, US Geological Survey Professional Paper 1360, p. 127-150.

Hitchcock, C.S., and Kelson, K.I., 2007, GIS-based liquefaction potential and effects mapping, Albuquerque-Santa Fe corridor, New Mexico: Final Technical Report, U.S. Geological Survey NEHRP, Award 03-HQ-GR-0067, 26 p. plus plates.

Holzer, T.L., Bennett, M.J., Noce, T.E., Padovani, A.C., and Tinsley, J.C., III, 2002, Liquefaction hazard and shaking amplification maps of Alameda, Berkeley, Emeryville, Oakland, and Piedmont: A digital database: U.S. Geological Survey Open-File Report 02-296, http://geopubs.wr.usgs.gov/open-file/of02-296.

Holzer, T.L., Bennett, M.J., Noce, T.E., and Tinsley, J.C., III, 2005, Shear wave velocity of surficial geologic sediments in Northern California: Statistical distributions and depth dependence: Earthquake Spectra, v. 21, no. 1, p. 161-177.

International Code Council (ICC), 2000, International Building Code 2000.

Joyner, W.B., and Fumal, T.E., 1985, Predictive mapping of earthquake ground motion: U.S. Geological Survey Professional Paper 1360, p. 203-220.

Kelson, K.I., Hitchcock, C.S., and Randolph, C.E., 1999, Liquefaction susceptibility in the Inner Rio Grande Valley near Albuquerque, New Mexico: Final Technical Report, U.S. Geological Survey NEHRP, Award 98-HQ-GR-1009, 40 p. plus appendices.

Louie, J.N., 2001, Faster, better: shear wave velocity to 100 meters depth from refraction microtremor arrays: Bulletin of the Seismological Society of America, v. 91, p. 347-364.

Louie, J.N., 2008, Shear wave velocity map for California: Collaborative Research with CGS, and UNR: Final Technical Report submitted to the U.S. Geological Survey NEHRP, Award 07-HQ-GR-0029, 98 p.

Machette, M.N., 2008, Paleoseismologic lessons learned—a 30-year perspective from the Rio Grande rift and Basin and Range province: Seismological Research Letters, v. 79, no. 2, p. 275.

Machette, M.N., Haller, K.L., and Wald, L., 2004, Quaternary Fault and Fold Database for the Nation: U.S. Geological Survey Fact Sheet 2004-3033.

Machette, M.N., Personius, S.F., Kelson, K.I., Haller, K.M., and Dart, R.L., 1998, Map of Quaternary faults and folds in New Mexico and adjacent areas: US Geological Survey Open-File Report 98-0521, scale 1:750,000.

McCalpin, J.P., 2008, Paleoseismic studies in the Rio Grande Rift, 1978-2008: Seismological Research Letters, v. 79, no. 2, p. 275.

MCEER, 2010, How Earthquakes Affect Buildings; MCEER State University of New York at Buffalo, viewed 10th October 2010, < http://mceer.buffalo.edu/infoservice/reference_services/EQaffectBuilding.asp>

National Earthquake Hazard Reduction Program (NEHRP), 1994, Recommended provisions for the development of Seismic Regulations for New Buildings, prepared by Building Seismic Safety Council for Federal Emergency Management Agency, Washington, D.C.

O'Connell, D.R.H., 2007, Concrete dams as seismic imaging sources: Geophysical Research Letters, v. 34, L20307, doi:10.1029/2007GL031219.

O'Connell, D.R.H, and Turner, J.P., 2010, Interferometric Multichannel Analysis of Surface Waves (IMASW), (Submitted, Reviewed), Bulletin of Seismological Society of America

Park, C.B., Miller, R.D., and Xia, J., 1999, Multimodal analysis of high frequency surface waves: Proceedings of the symposium on the application of geophysics to engineering and environmental problems '99, p. 115-121.

Park, S., and Elrick, S., 1998, Predictions of shear wave velocities in southern California using surface geology, Bulletin of the Seismologic Society of America, v. 88, n. 3, p. 677-685.Aydin, A., 1982, The East Bay Hills, a compressional domain resulting from interaction between the Calaveras and Hayward-Rodgers Creek faults: California Division of Mines and Geology Special Publication 62, p.11-22.

Personius, S.F., Machette, M.N., and Kelson, K.I., 1999, Quaternary faults in the Albuquerque area—an update: New Mexico Geological Society Guidebook 50, p. 189-200.

Personius, S.F., Eppes, M.C., Mahan, S.A., Love, D.W., Mitchell, D.K., and Murphy, A., 2001, Log and data from a trench across the Hubbell Springs fault zone, Bernalillo County, New Mexico: U.S. Geological Survey Miscellaneous Field Studies Map MF-2348, v. 1.1.

Petersen, M.D., Frankel, A.D., Harmsen, S.C., Mueller, C.S., Haller, K.M., Wheeler, R.L., Wesson, R.L., Zeng, Y., Boyd, O.S., Perkins, D.M., Luco, N., Field, E.H., Wills, C.J., and Rukstales, K.S., 2008, Documentation for the 2008 update of the United States national seismic hazard maps: U.S. Geological Survey Open-File Report 2008-1128, 61 p.

Scott, J.B., Clark, M., Rennie, T., Pancha, A., Park, H., and Louie, J.N., 2004, A shallow shear wave velocity transect across the Reno, Nevada area basin: Bulletin of the Seismological Society of America, v. 94, no. 6, p. 2,222-2,228.

Scott, J.B., Rasmussen, T., Luke, B., Taylor, W.J., Wagoner, J.L., Smith, S.B., and Louie, J.N., 2006, Shallow shear velocity and seismic microzonation of the urban Las Vegas, Nevada basin: Bulletin of the Seismological Society of America, v. 96, no. 3, p. 1,068-1,077.

Stephenson, W.J., Louie, J.N., Pullammanappallil, S., Williams, R.A., and Odum, J.K., 2005, Blind shear wave velocity comparison of ReMi and MASW results with boreholes to 200 m in Santa Clara Valley: implications for earthquake ground motion assessment: Bulletin of the Seismological Society of America, v. 95, no. 6, p. 2,506-2,516.

Thelen, W.A, Clark, M., Lopez, C.T., Loughner, C., Park, H., Scott, J.B., Smith, S.B., Greschke, R., and Louie, J.N., 2006, A transect of 200 shallow shear velocity profiles across the Los Angeles Basin: Bulletin of the Seismological Society of America, v. 96, no. 3, p. 1,055-1,067.

Williams, P.L., and Cole, J.C., compilers, 2007, Geologic map of the Albuquerque 30-minute x 60-minute quadrangle, north-central New Mexico: U.S. Geological Survey Scientific Investigations Map 2946, 31 p. plus plate, scale 1:100,000.

Wills, C.J., and Clahan, K.B., 2006, Developing a map of geologically defined site-condition categories for California: Bulletin of the Seismological Society of America, v. 96, no. 4A, p. 1,483-1,501.

Wills, C.J., and Gutierrez, C., 2008, Investigation of geographic rules for improving site-conditions mapping: Final Technical Report submitted to the U.S. Geological Survey NEHRP, Award 07-HQ-GR-0061, 20 p.

Wills, C.J., Petersen, M.D., Bryant, W.A., Reichle, M.S., Saucedo, G.J., Tan, S.S., Taylor, G.C., and Treiman, J.A., 2000, A site conditions map for California based on geology and shear wave velocity: Bulletin of the Seismological Society of America, v. 90, no. 6b, p. S187-S208.

Wong, I., Olig, S., Dober, M., Silva, W., Wright, D., Thomas, P., Gregor, N., Sanford, A., Lin, K., and Love, D., 2004, Earthquake scenario and probabilistic ground-shaking hazard maps for the Albuquerque-Belen-Santa Fe, New Mexico, corridor: New Mexico Geology, v. 26, no. 1, p. 3-33.

U.S. Geological Survey (USGS) and New Mexico Bureau of Mines and Mineral Resources (NMBMMR), 2006, Quaternary fault and fold database for the United States, accessed May 2, 2008, from USGS web site: http//earthquake.usgs.gov/regional/qfaults/.

Zachariasen, J.A., Olig, S.S., 2008, A longer, wider Hubbell Spring fault system with footwall backtilting: typical or atypical fault in the Rio Grande rift: Seismological Research Letters, v. 79, no. 2, p. 275.

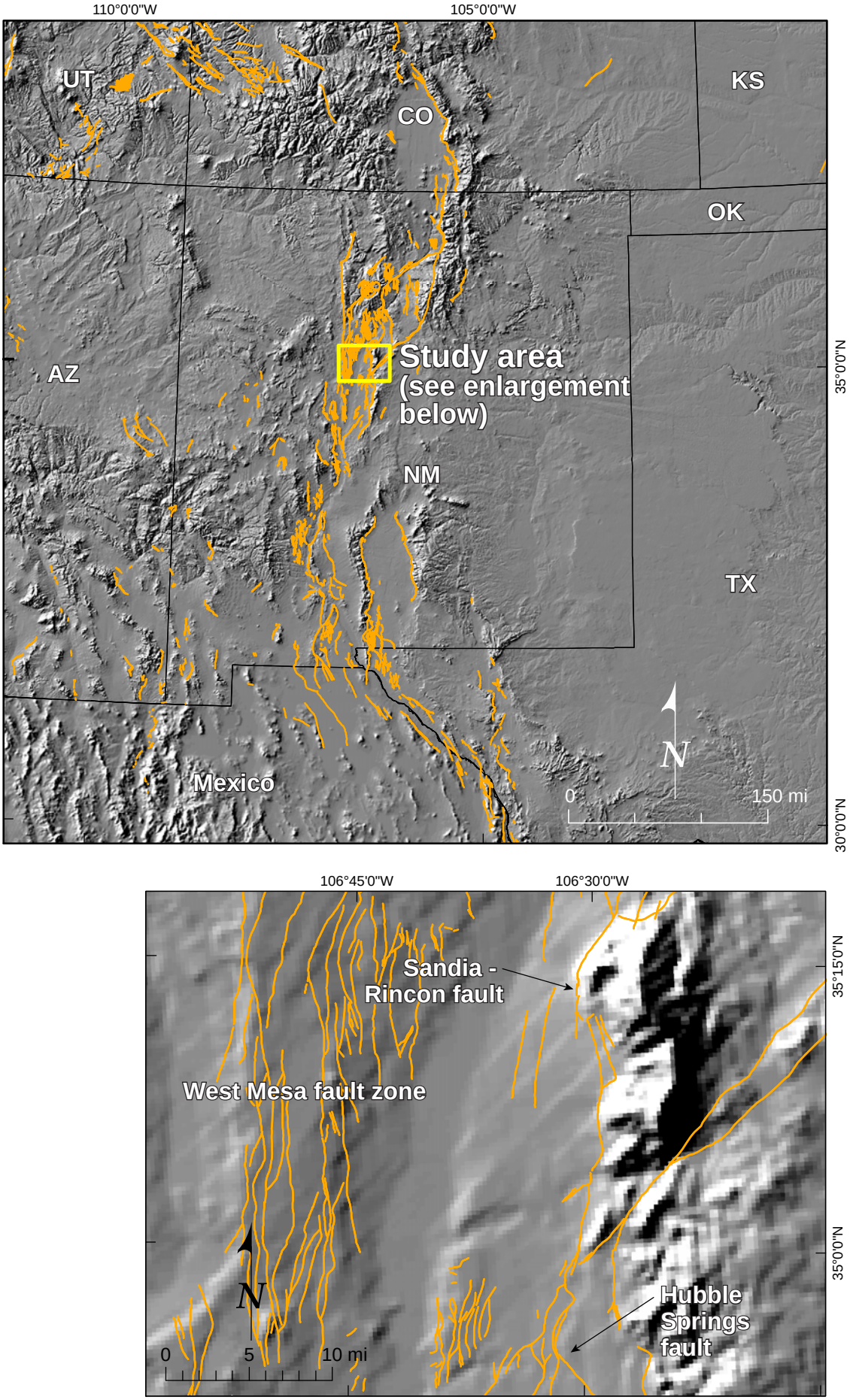

GRAPHICS, Projects 2068, ABQ NEHRP, modified 12.01.10

Figure 1. Location map

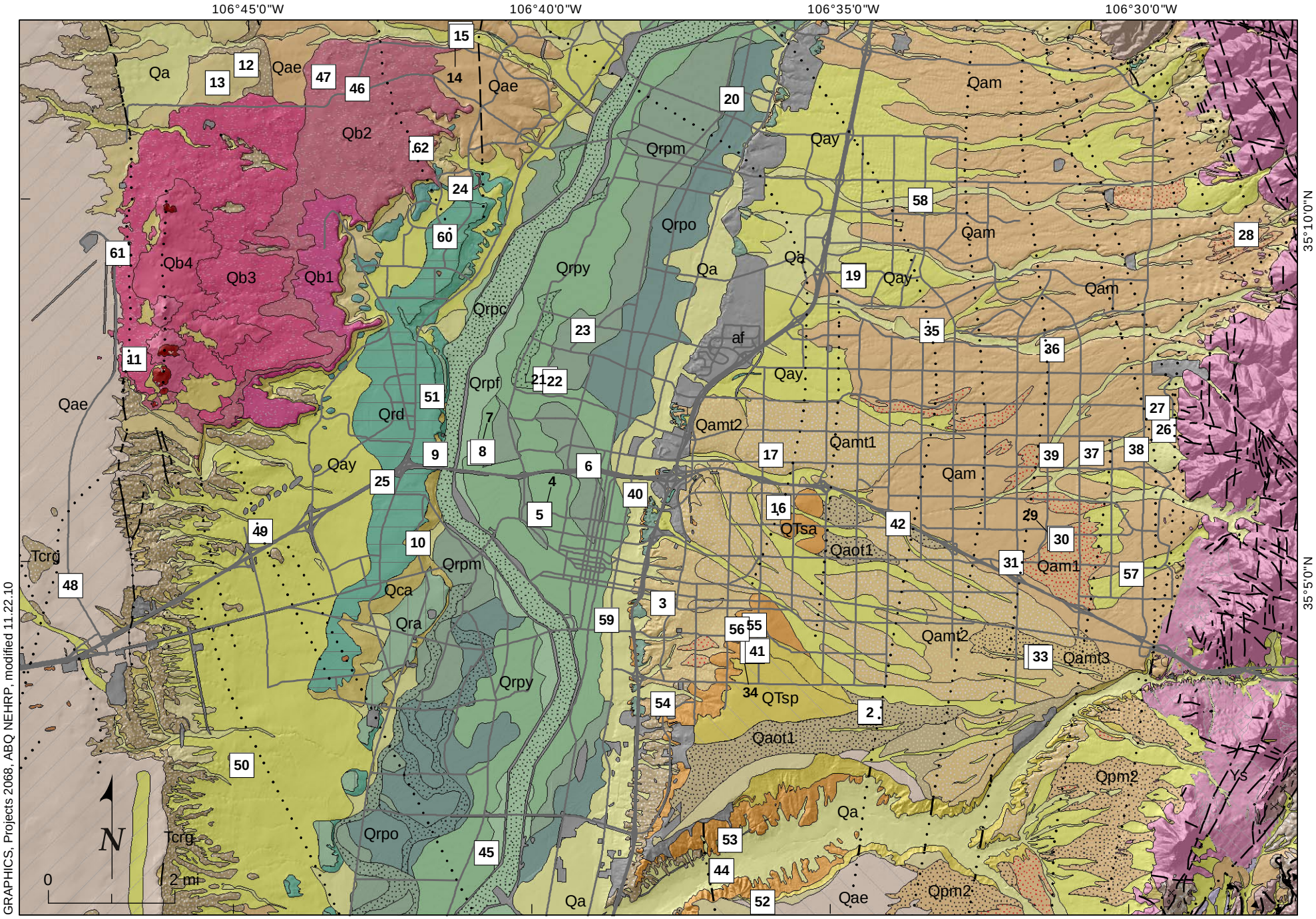

Figure 2a. Geologic map and IMASW survey locations

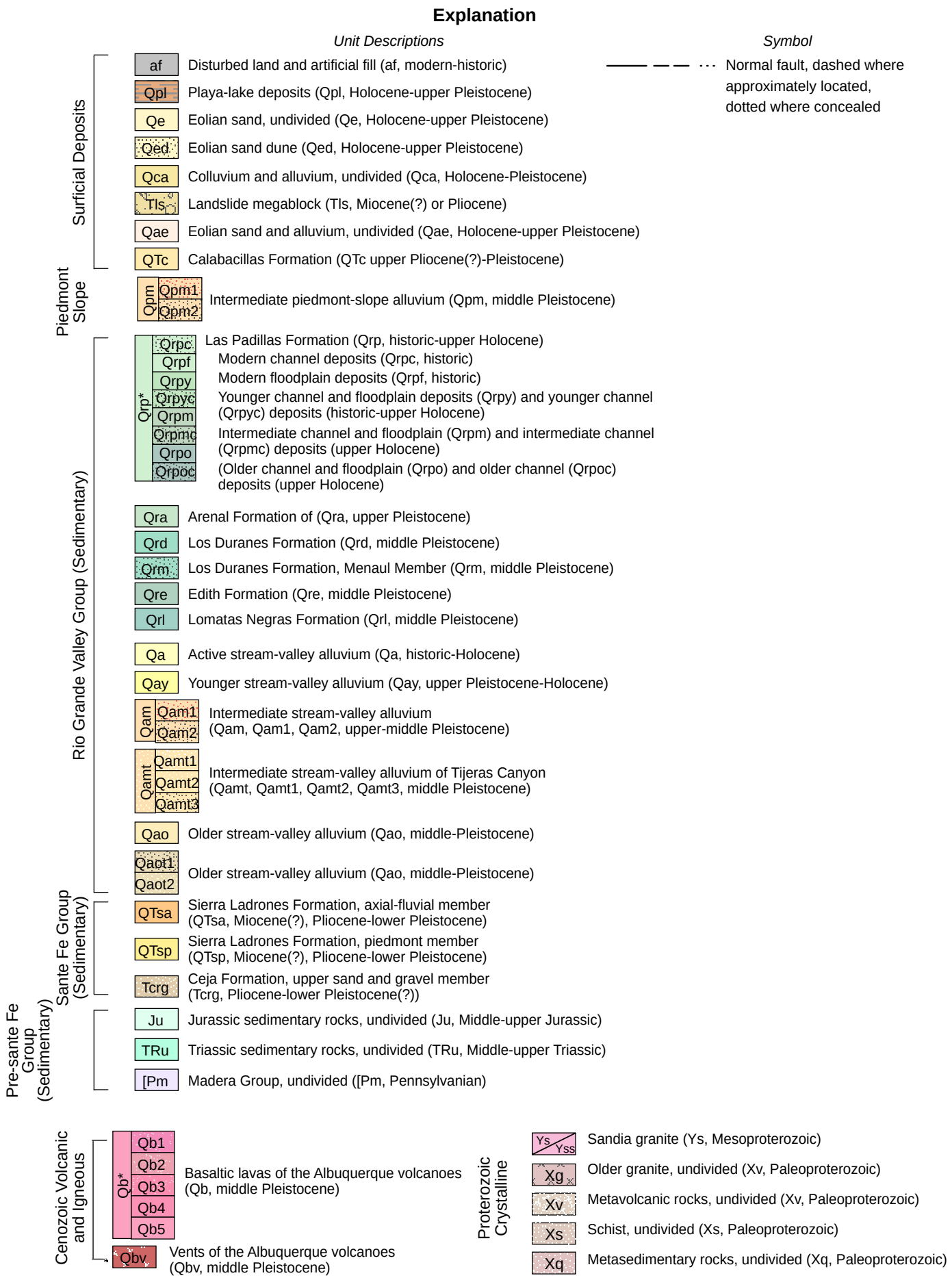

Figure 2b. Geologic map explanation (from Connell, 2006)

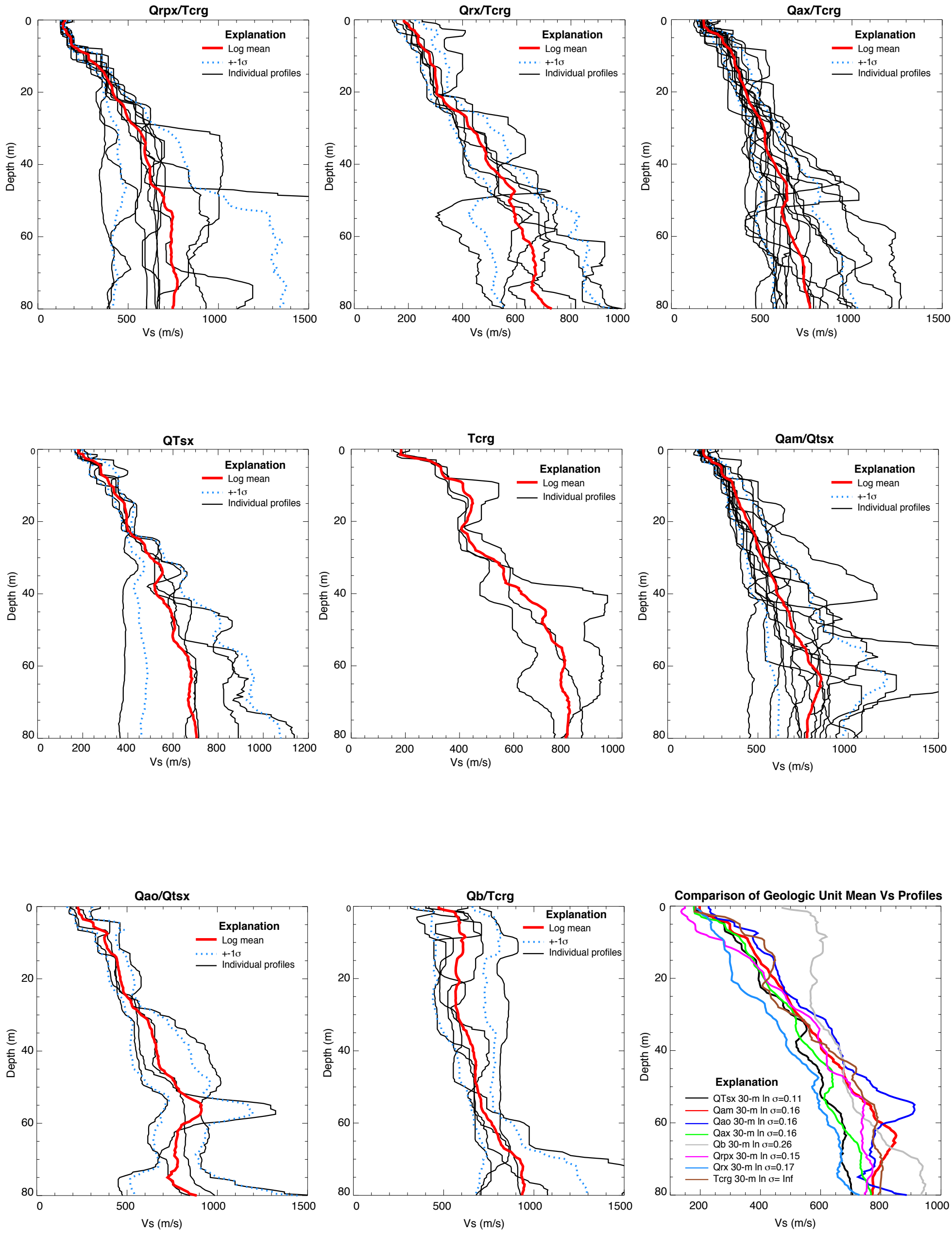

Figure 3. Composite Vs-Structure Plots. IMASW-based Vs profiles are depicted by black lines and organized by the surficial geologic unit at each survey site. Underlying geologic units are depicted in the labels; e.g. Qrpx/Tcrg indicates that Qrpx is the surficial unit that overlies Tcrg. Red lines depict log-mean composite Vs profiles calculated for each Vs-lithologic unit. The Comparison of Geologic Unit Mean Vs Profiles figure shows each log-mean composite Vs profile at the same scale for side-by-side comparison.

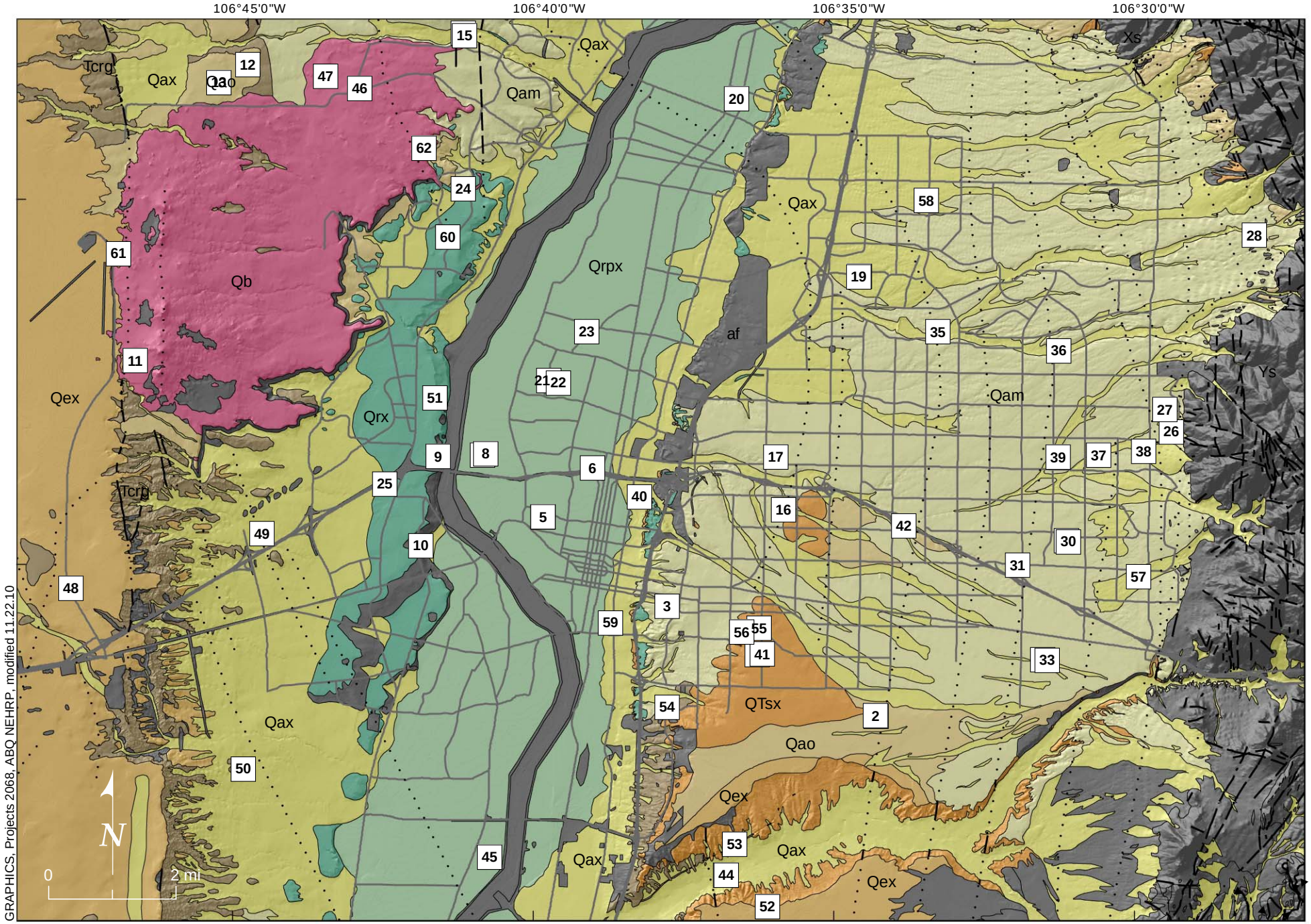

Geology from Connell, 2006

Figure 4a. Vs-lithology grouped geologic units

Explanation

Symbol

Normal fault, dashed where approximately located, dotted where concealed

Geologic Units

Unsampled units

Qa — Active stream-valley alluvium (Qa, historic-Holocene)
Younger stream-valley alluvium (Qay, upper Pleistocene-Holocene)

Qao — Older stream-valley alluvium (Qao, Qaot1, Qaot2, middle-Pleistocene)

Qex — Eolian sand, undivided (Qe, Holocene-upper Pleistocene)
Eolian sand and alluvium, undivided (Qae, Holocene-upper Pleistocene)

Qam — Intermediate stream-valley alluvium
(Qam, Qam1, Qam2, upper-middle Pleistocene)
(Qamt, Qamt1, Qamt2, Qamt3, upper-middle Pleistocene)

QTsx — Sierra Ladrones Formation (QTsa, QTsp, Miocene(?), Pliocene-lower Pleistocene)

Qrp — Las Padillas Formation (historic-upper Holocene)

Qrx — River-valley alluvium (Qra, Qrd, Qrm, Qre, Qrl, middle to upper Pleistocene)

Tcrg — Ceja Formation, upper sand and gravel member (Tcrg, Pliocene-lower Pleistocene(?))

Qb — Basaltic lavas of the Albuquerque volcanoes (Qb, middle Pleistocene)

Figure 4b. Explanation for Vs-lithology grouped map (modified from Connell, 2006)

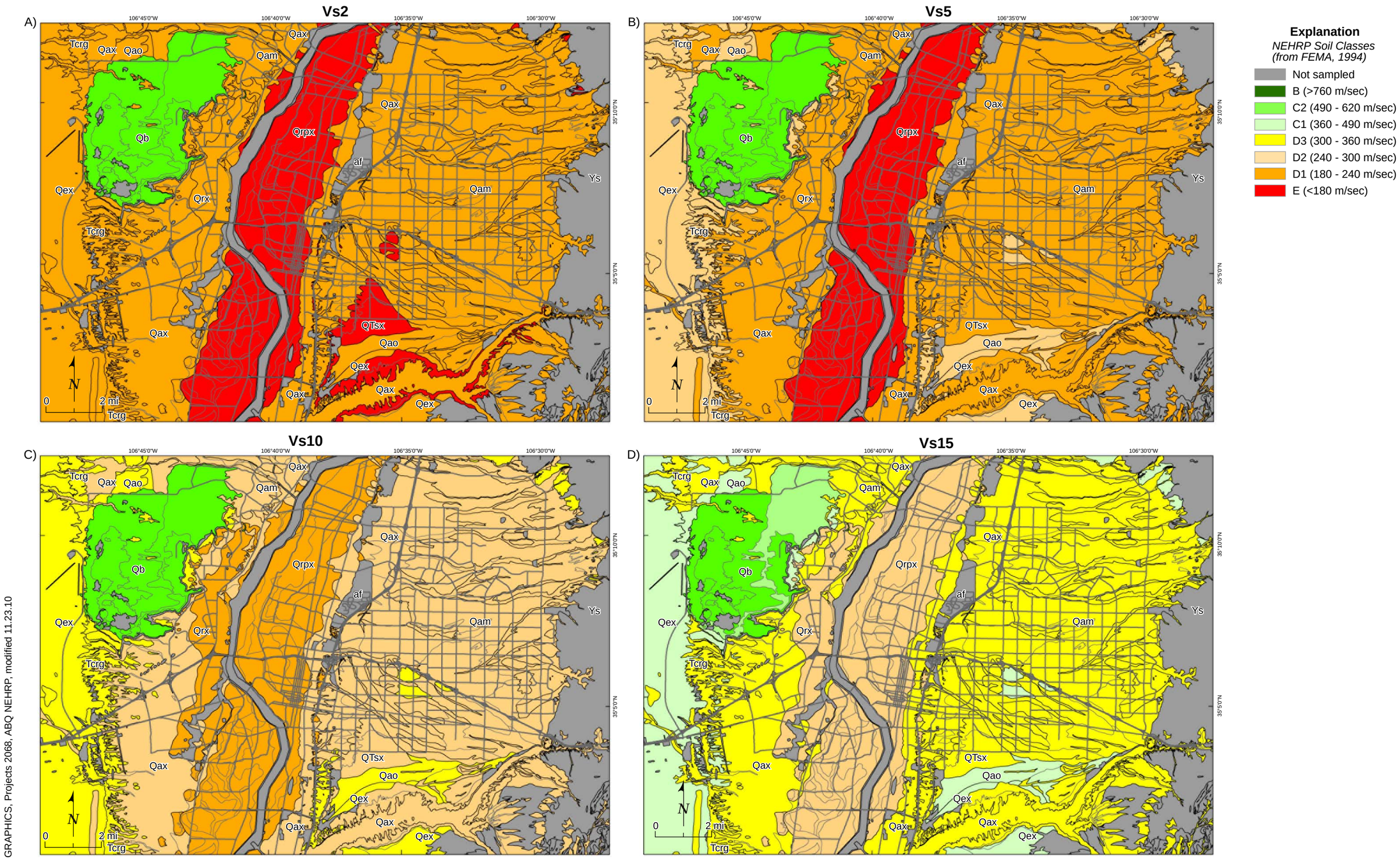

GRAPHICS, Projects 2068, ABQ NEHRP, modified 11.23.10

Figure 5. Classification maps

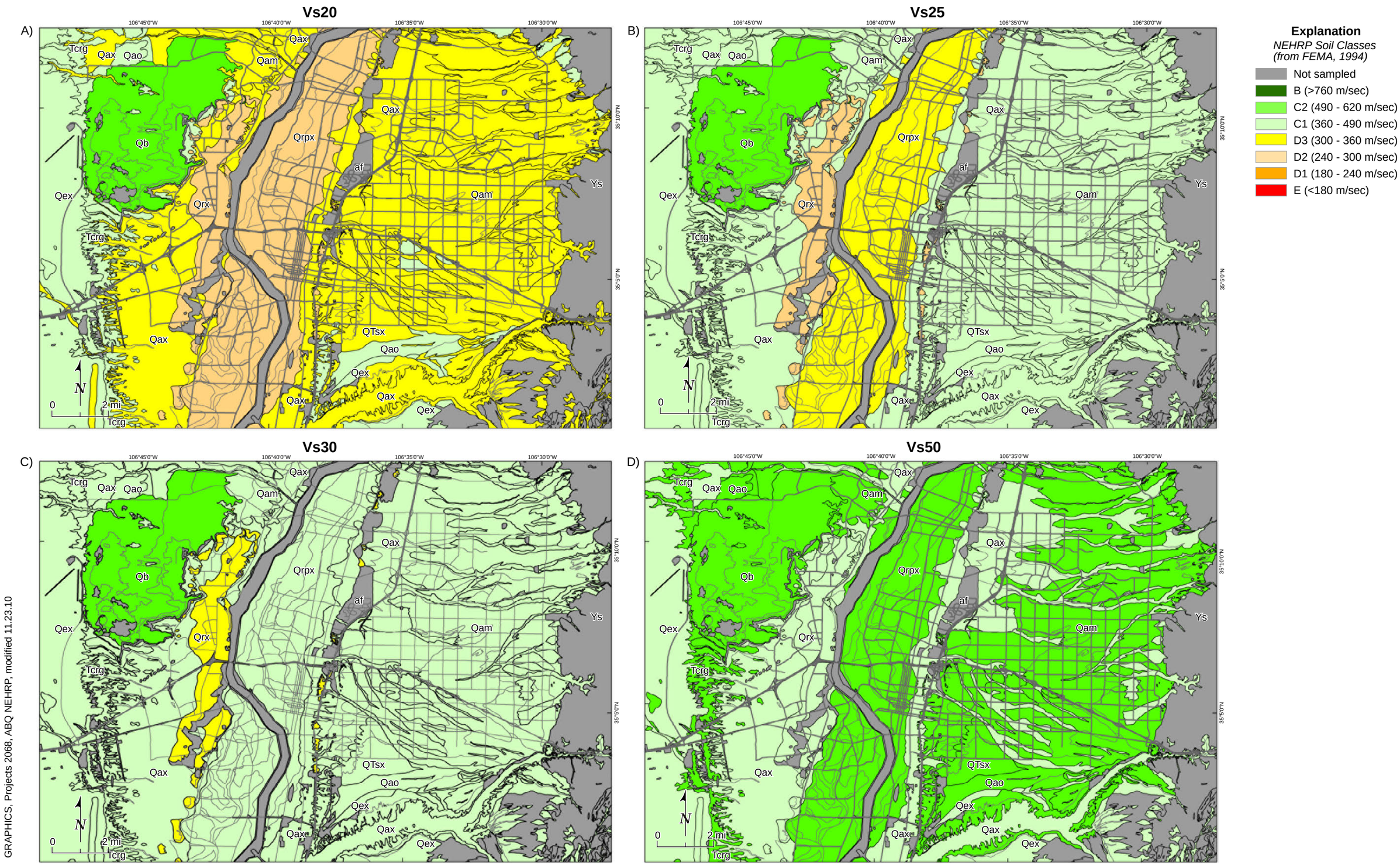

GRAPHICS, Projects 2068, ABQ NEHRP, modified 11.23.10

Figure 6. Classification maps

A)

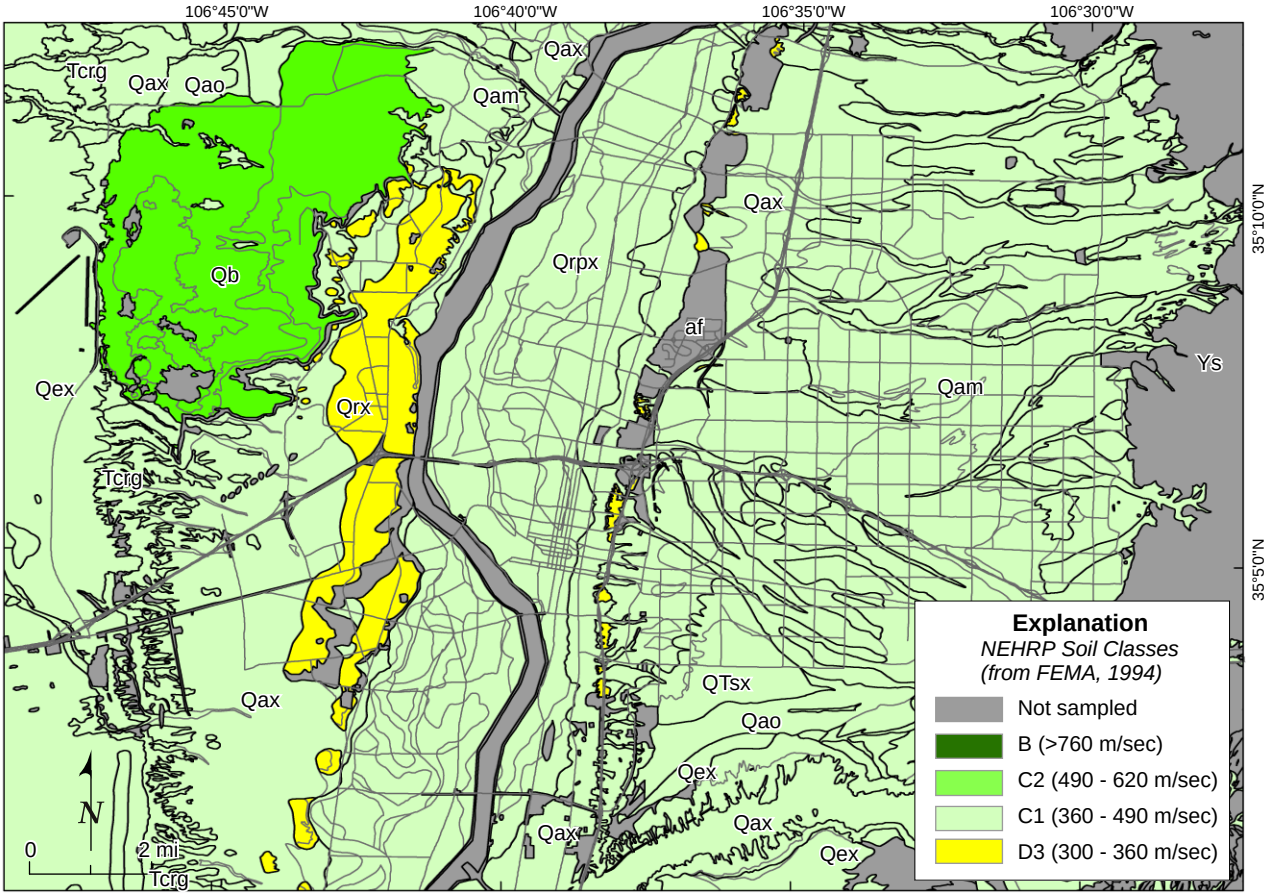

B)

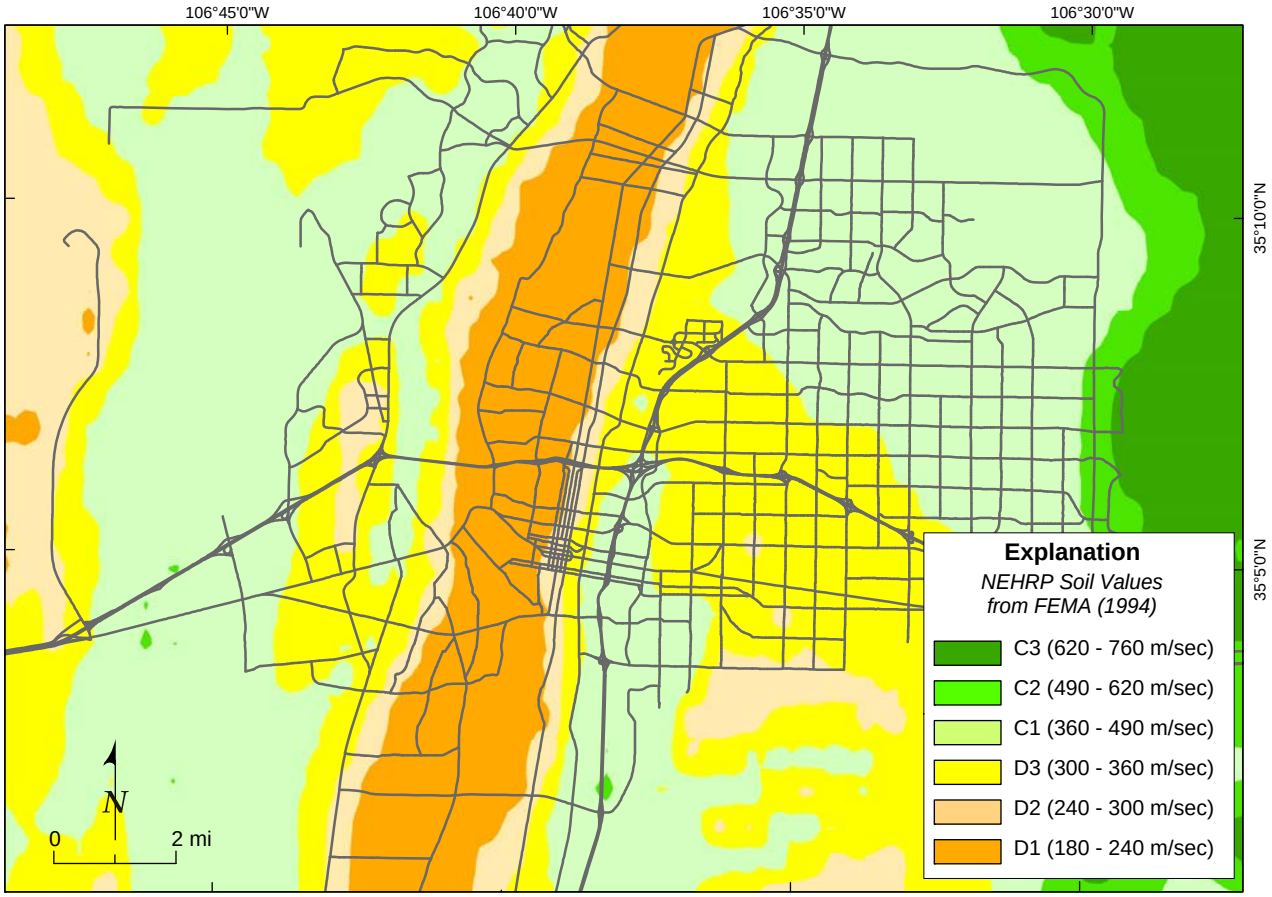

Figure 7. Comparison: (A) IMASW Vs30 vs (B) USGS Mapserver Vs30

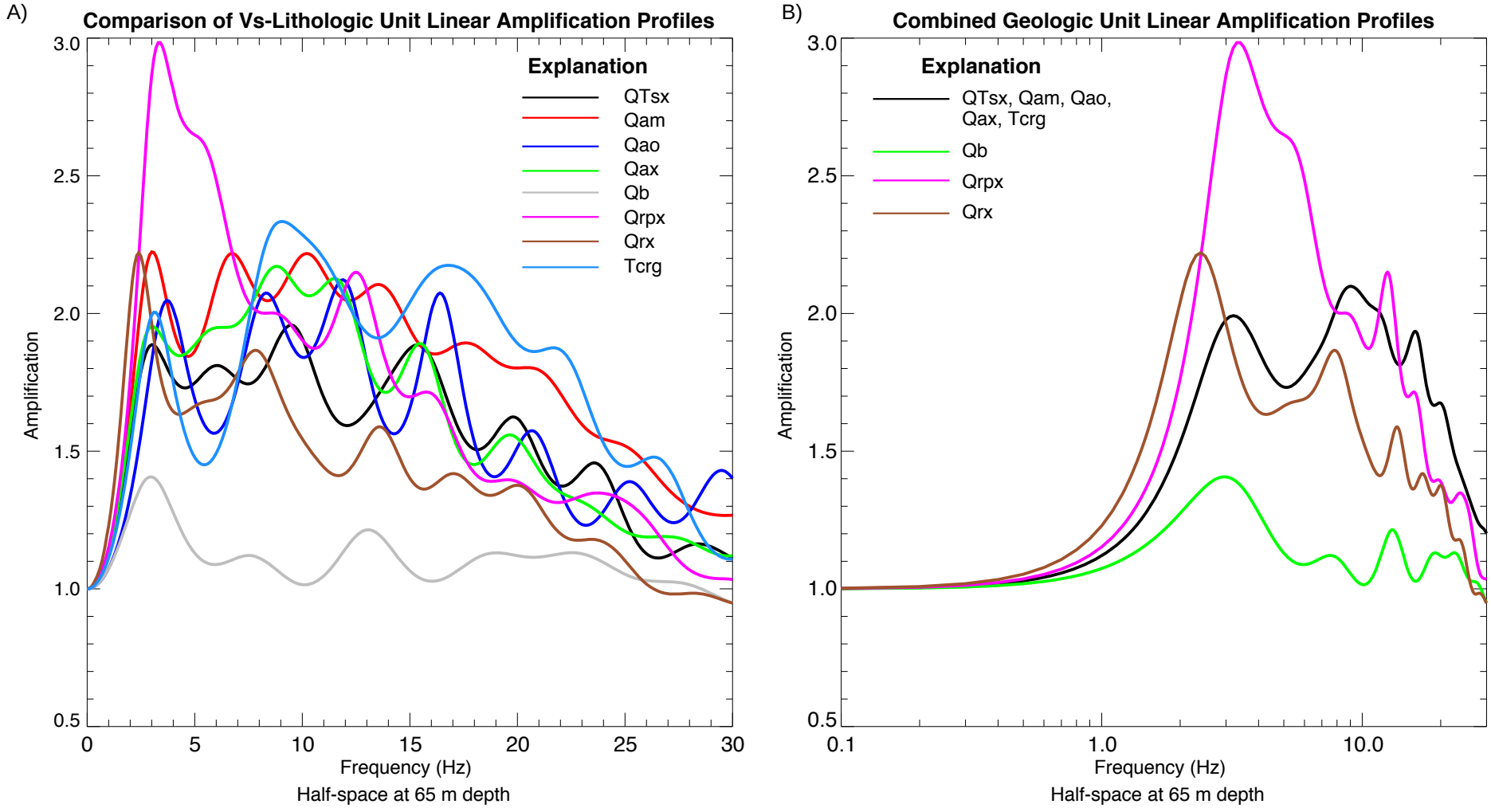

Figure 8. Shallow amplification factors

8.0 APPENDICES

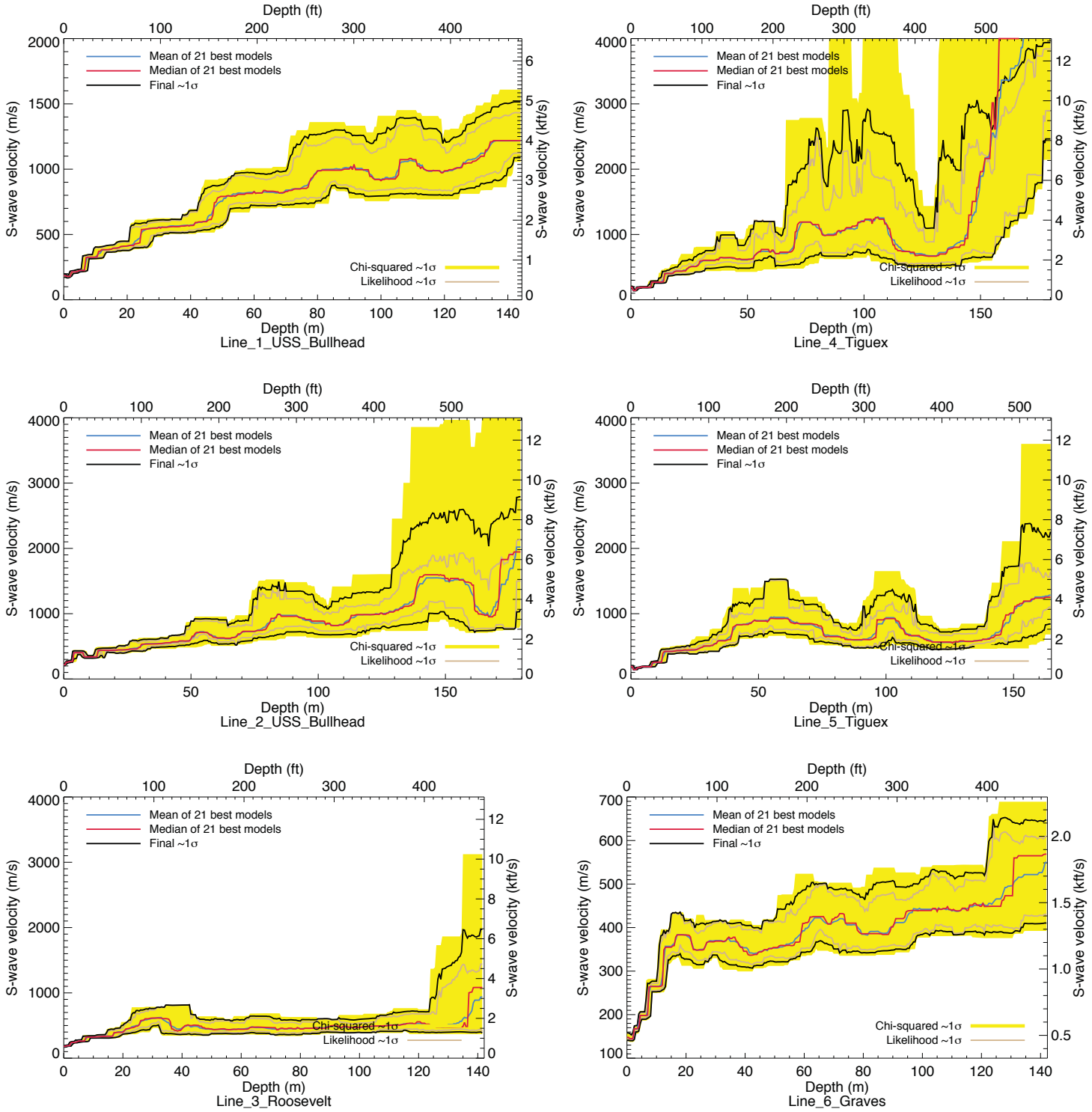

Figure A-1. S-wave velocities

GRAPHICS, Projects 2068, ABQ NEHRP, modified 11.23.10

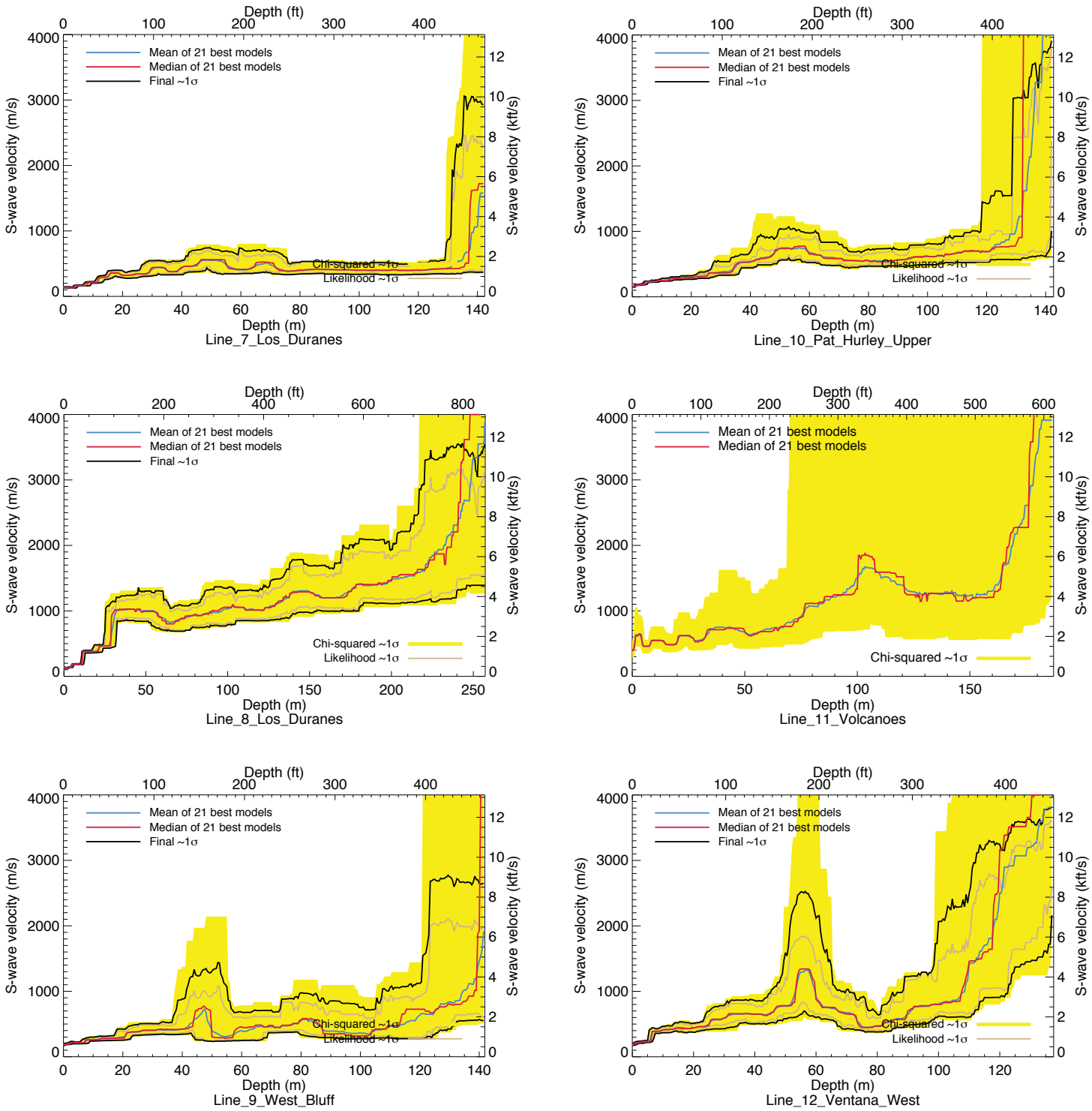

GRAPHICS, Projects 2068, ABQ NEHRP, modified 11.23.10

Figure A-2. S-wave velocities

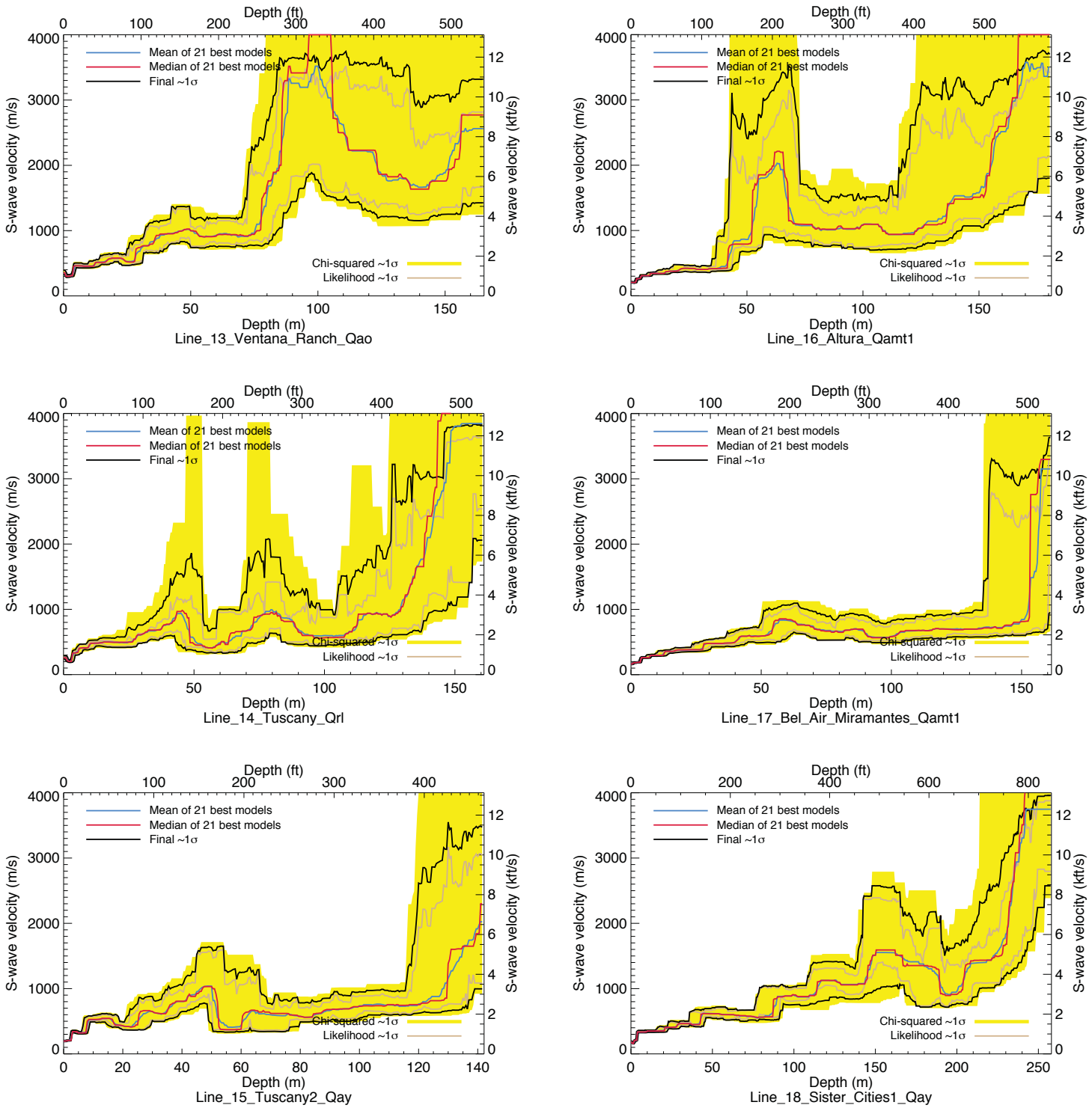

Figure A-3. S-wave velocities

GRAPHICS, Projects 2068, ABQ NEHRP, modified 11.23.10

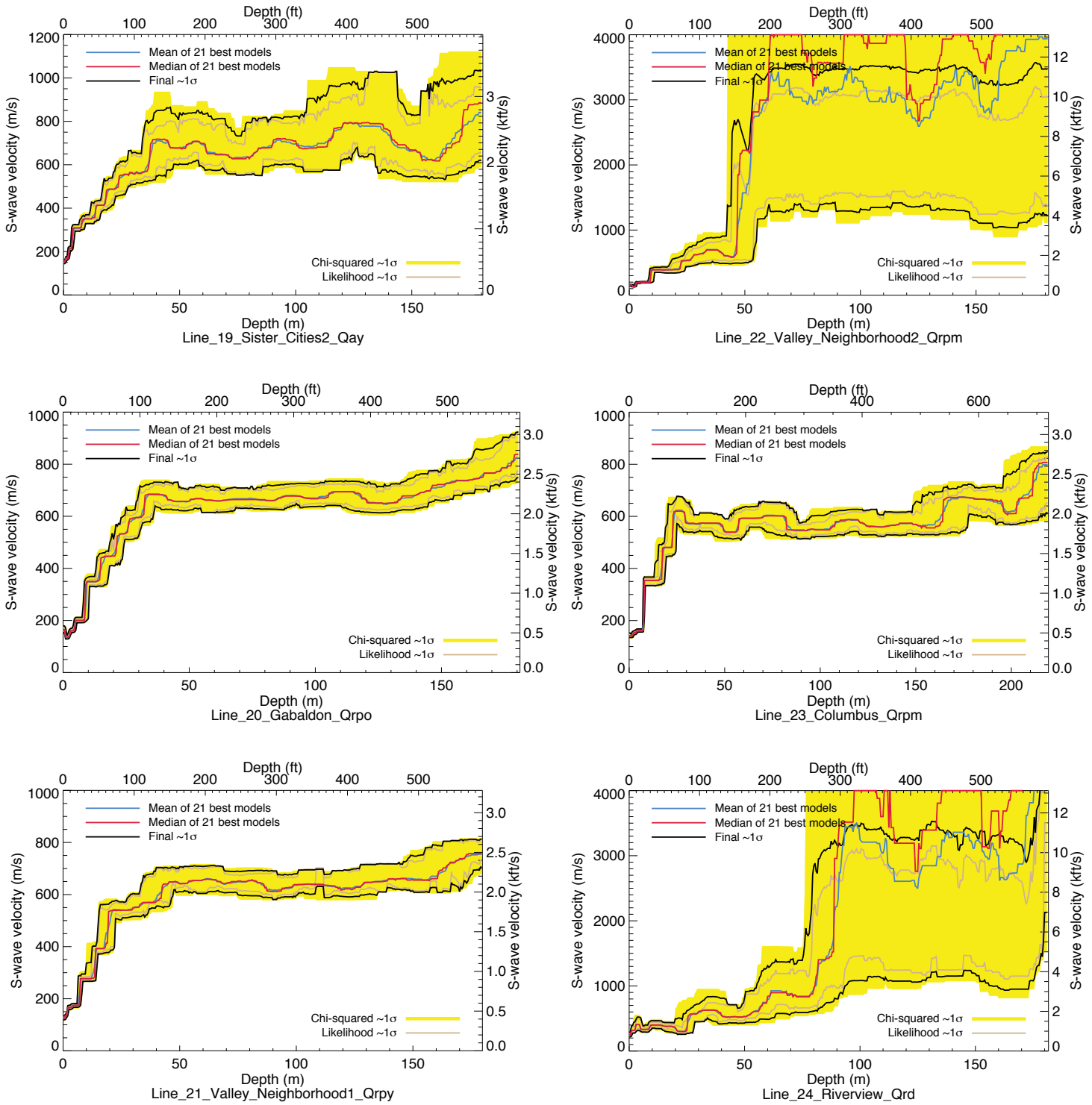

Figure A-4. S-wave velocities

GRAPHICS, Projects 2068, ABQ NEHRP, modified 11.23.10

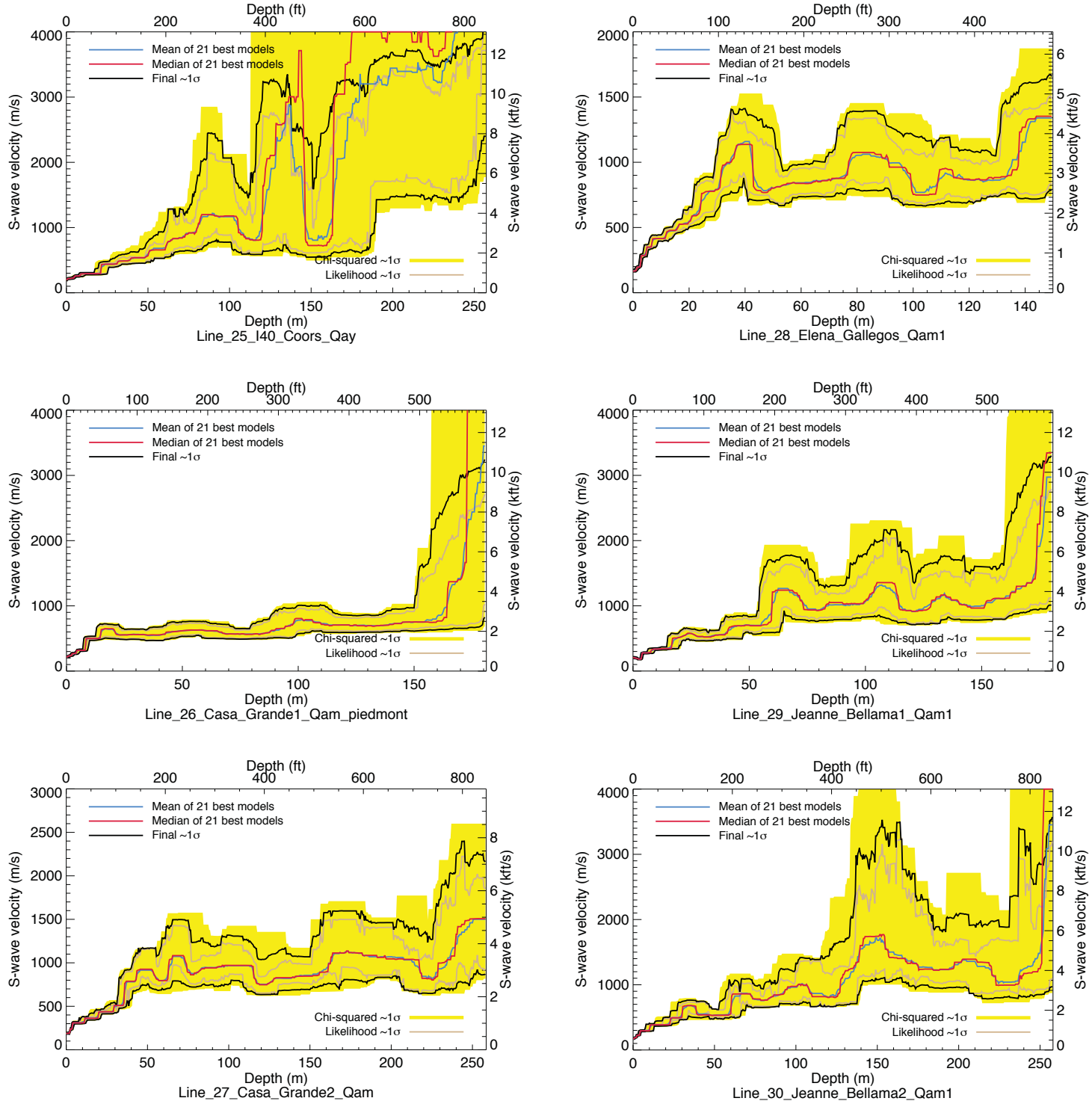

Figure A-5. S-wave velocities

GRAPHICS, Projects 2068, ABQ NEHRP, modified 11.23.10

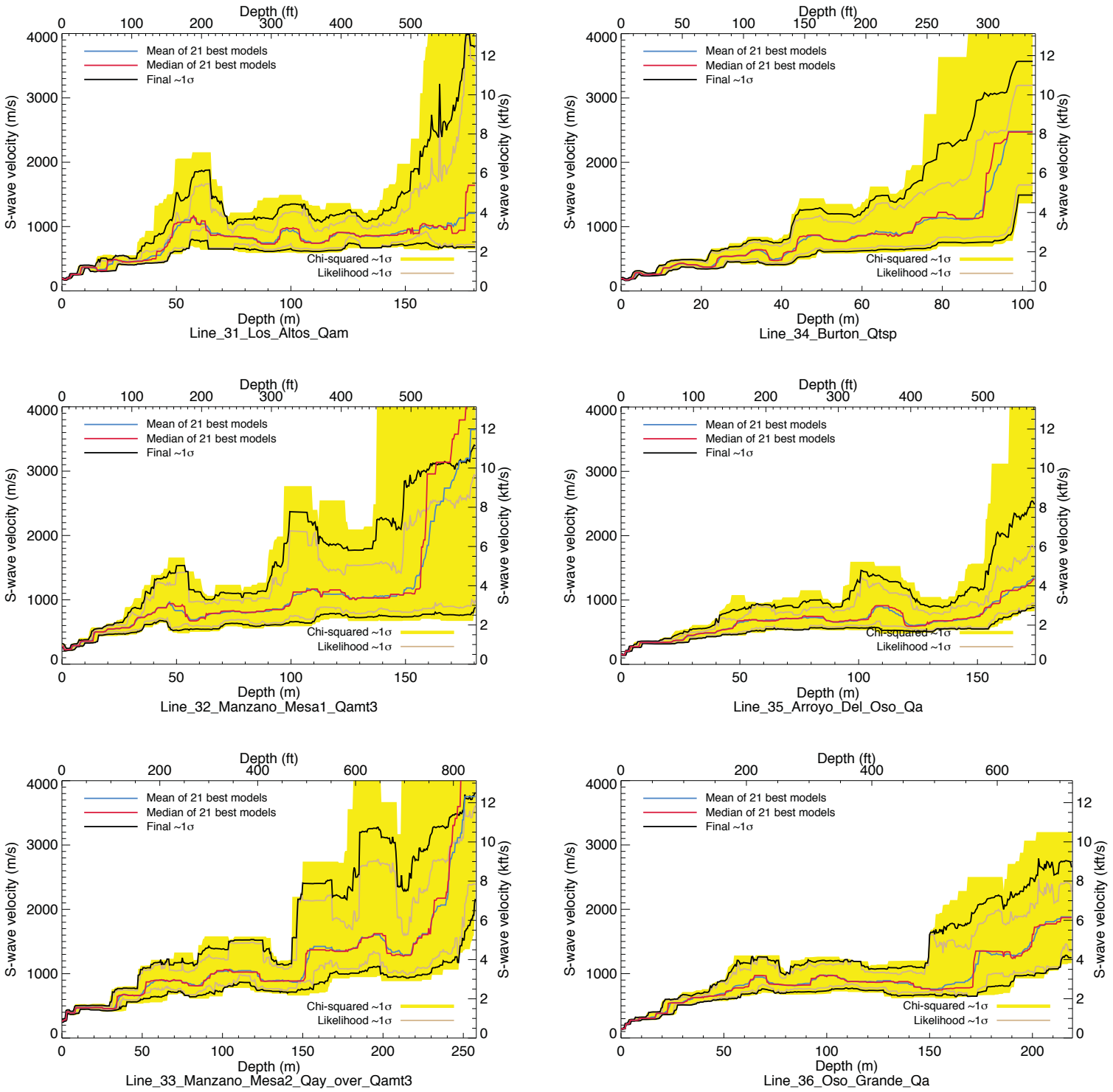

Figure A-6. S-wave velocities

GRAPHICS, Projects 2068, ABQ NEHRP, modified 11.23.10

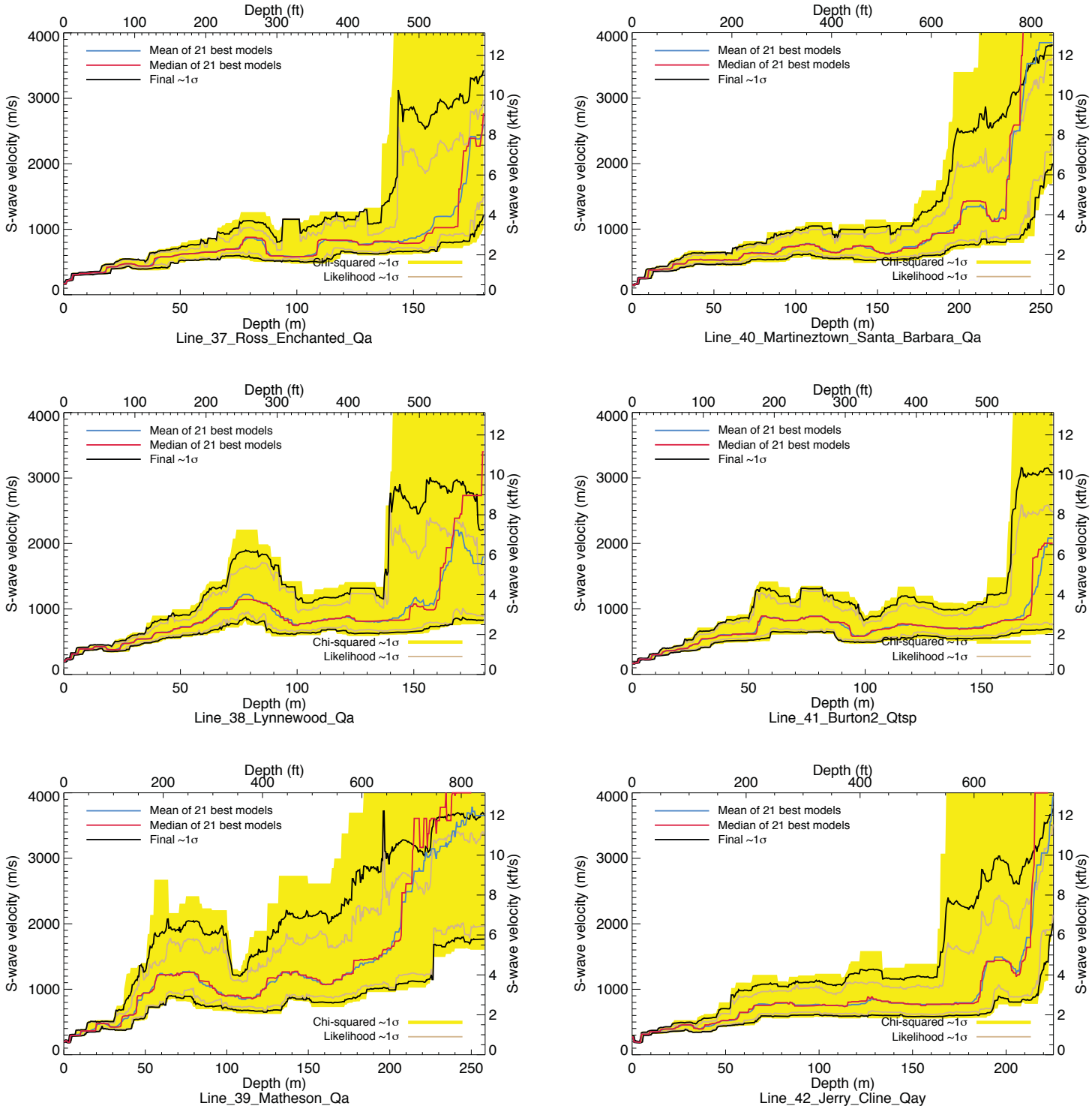

GRAPHICS, Projects 2068, ABQ NEHRP, modified 11.23.10

Figure A-7. S-wave velocities

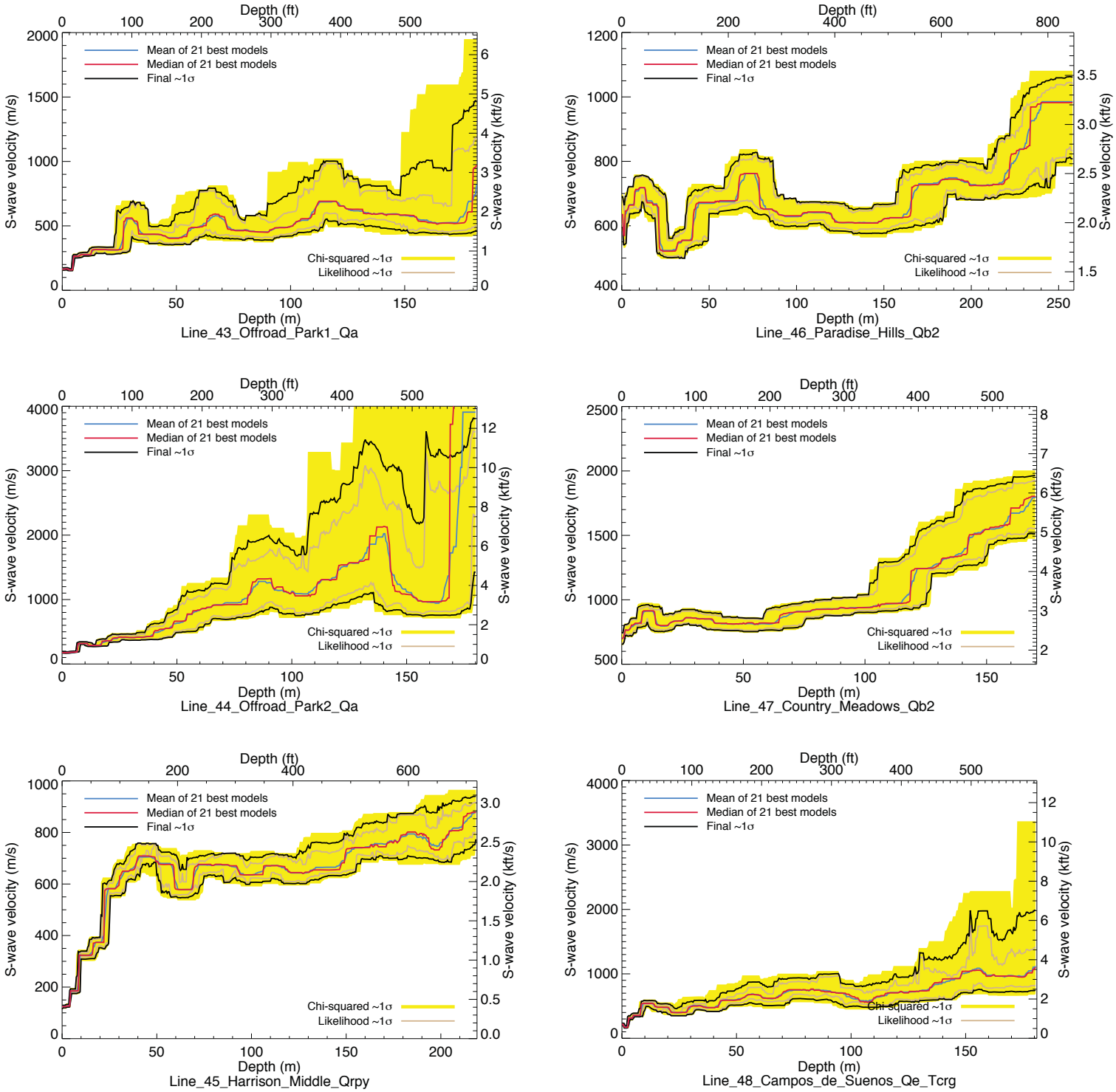

Figure A-8. S-wave velocities

GRAPHICS, Projects 2068, ABQ NEHRP, modified 11.23.10

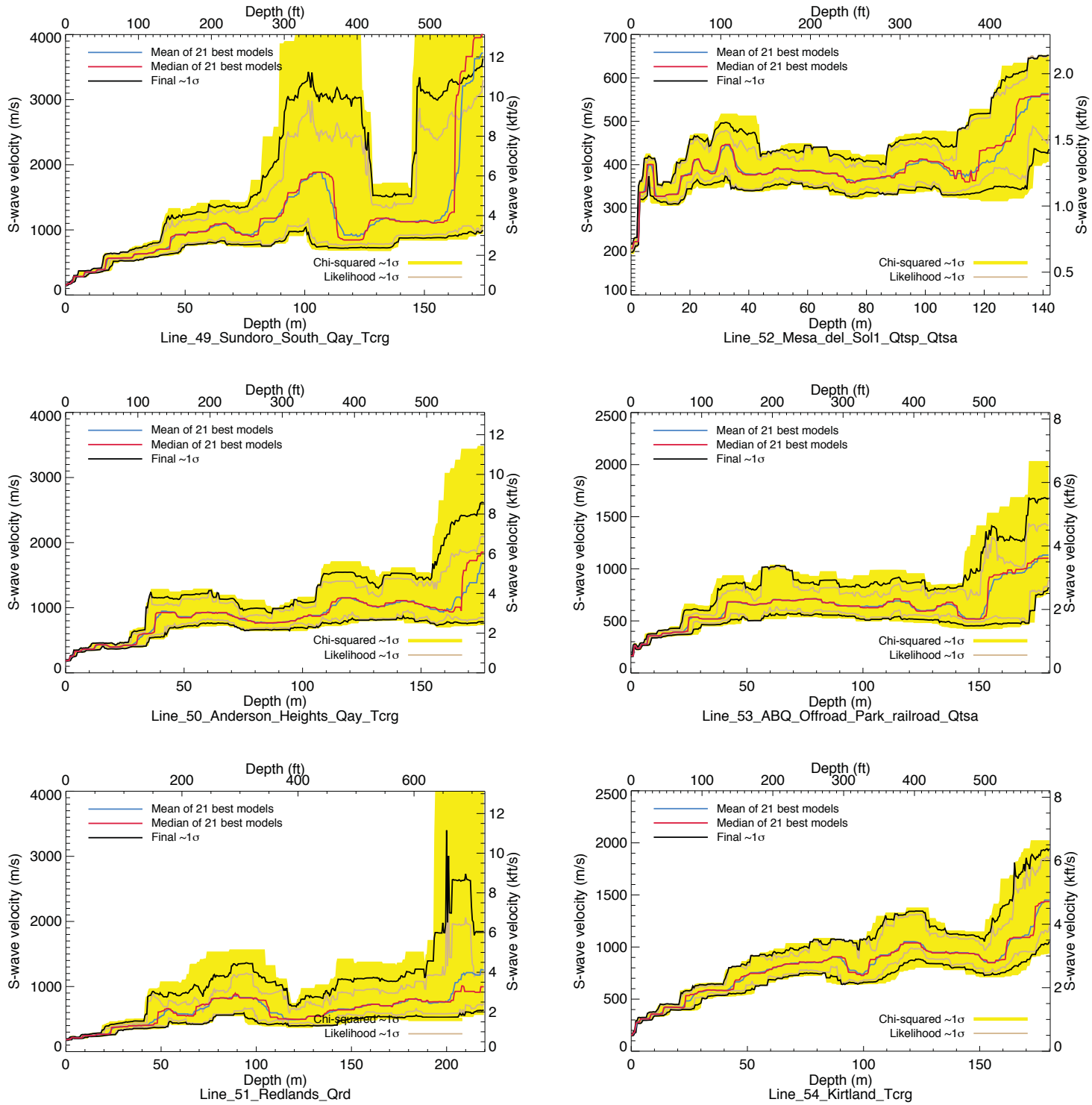

Figure A-9. S-wave velocities

GRAPHICS, Projects 2068, ABQ NEHRP, modified 11.23.10

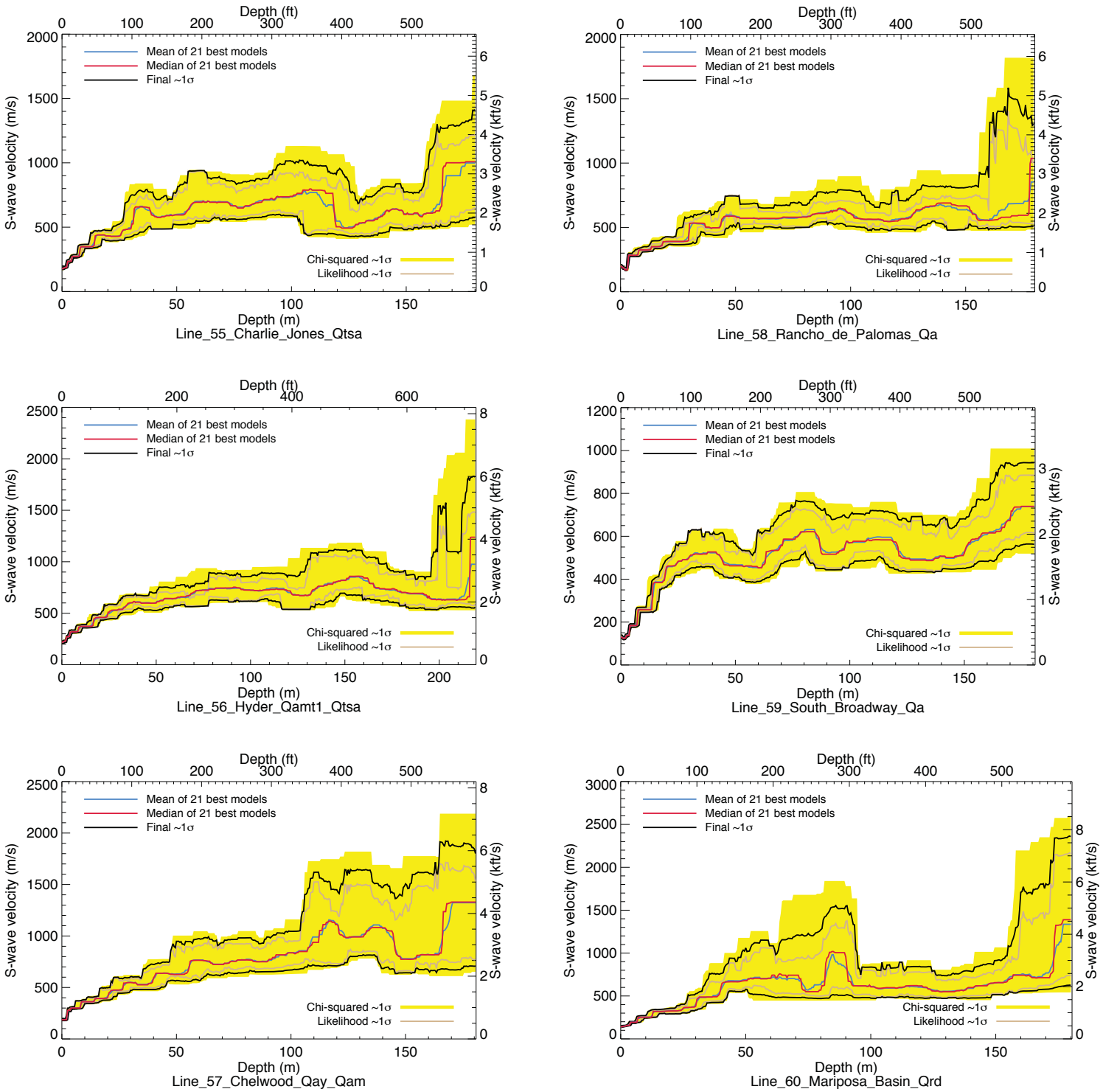

GRAPHICS, Projects 2068, ABQ NEHRP, modified 11.23.10

Figure A-10. S-wave velocities

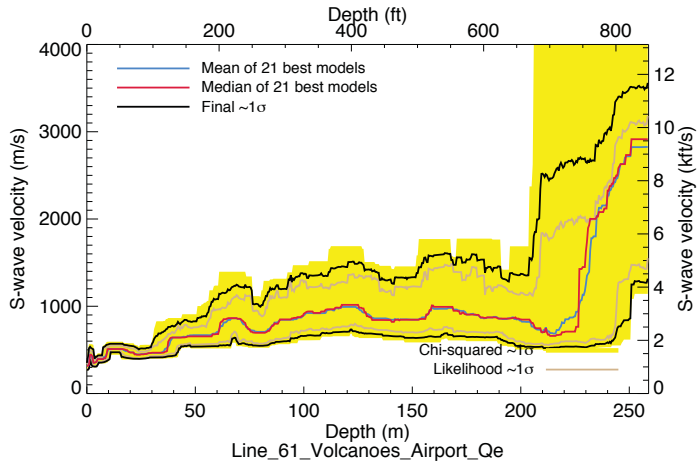

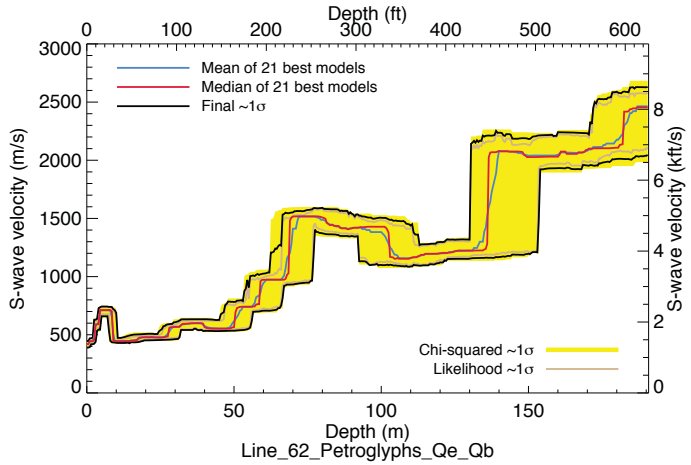

Figure A-11. S-wave velocities

GRAPHICS, Projects 2068, ABQ NEHRP, modified 11.23.10

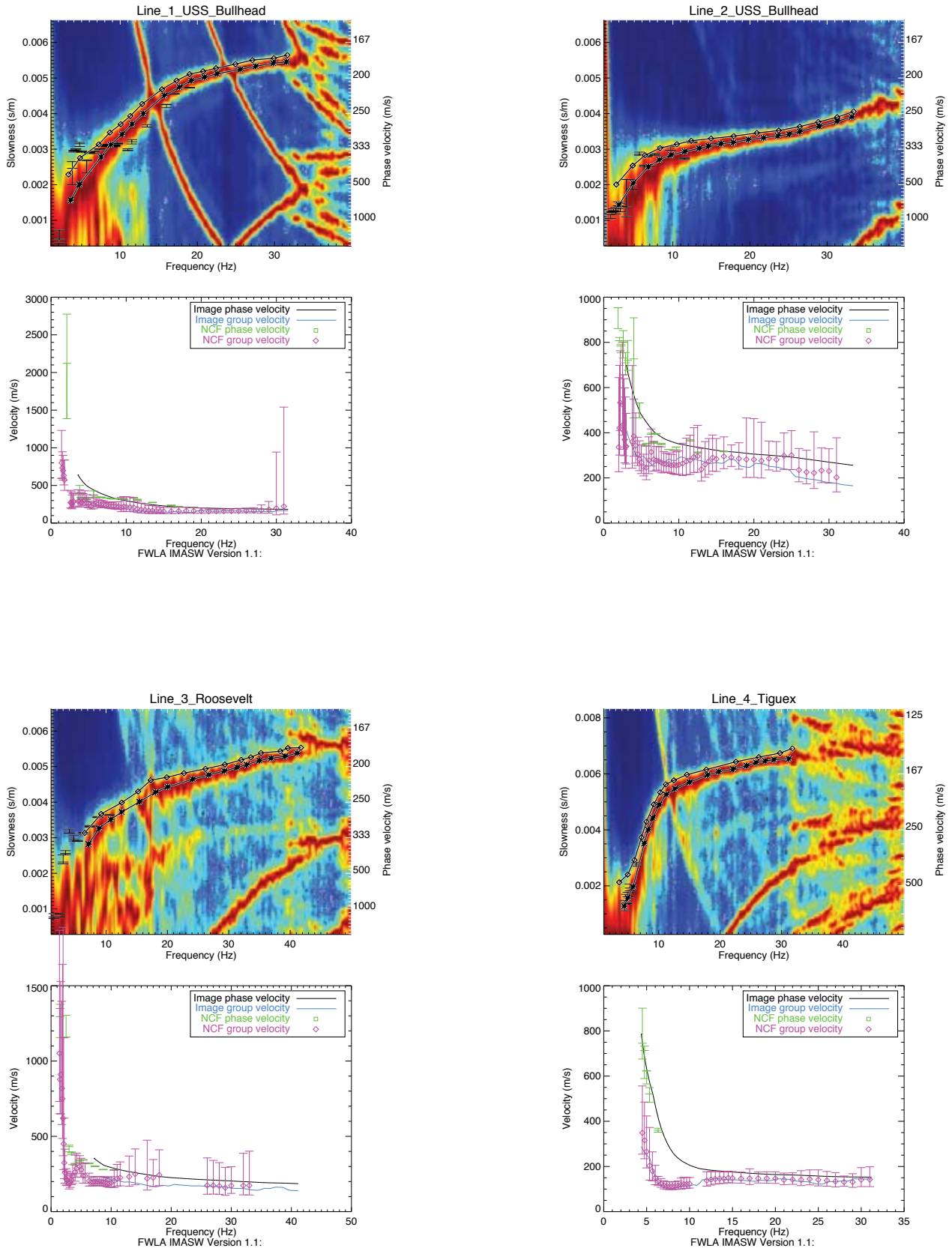

Figure B-1. Rayleigh-wave dispersion images with phase- and group-velocity picks

GRAPHICS, Projects 2068, ABQ NEHRP, modified 11.23.10

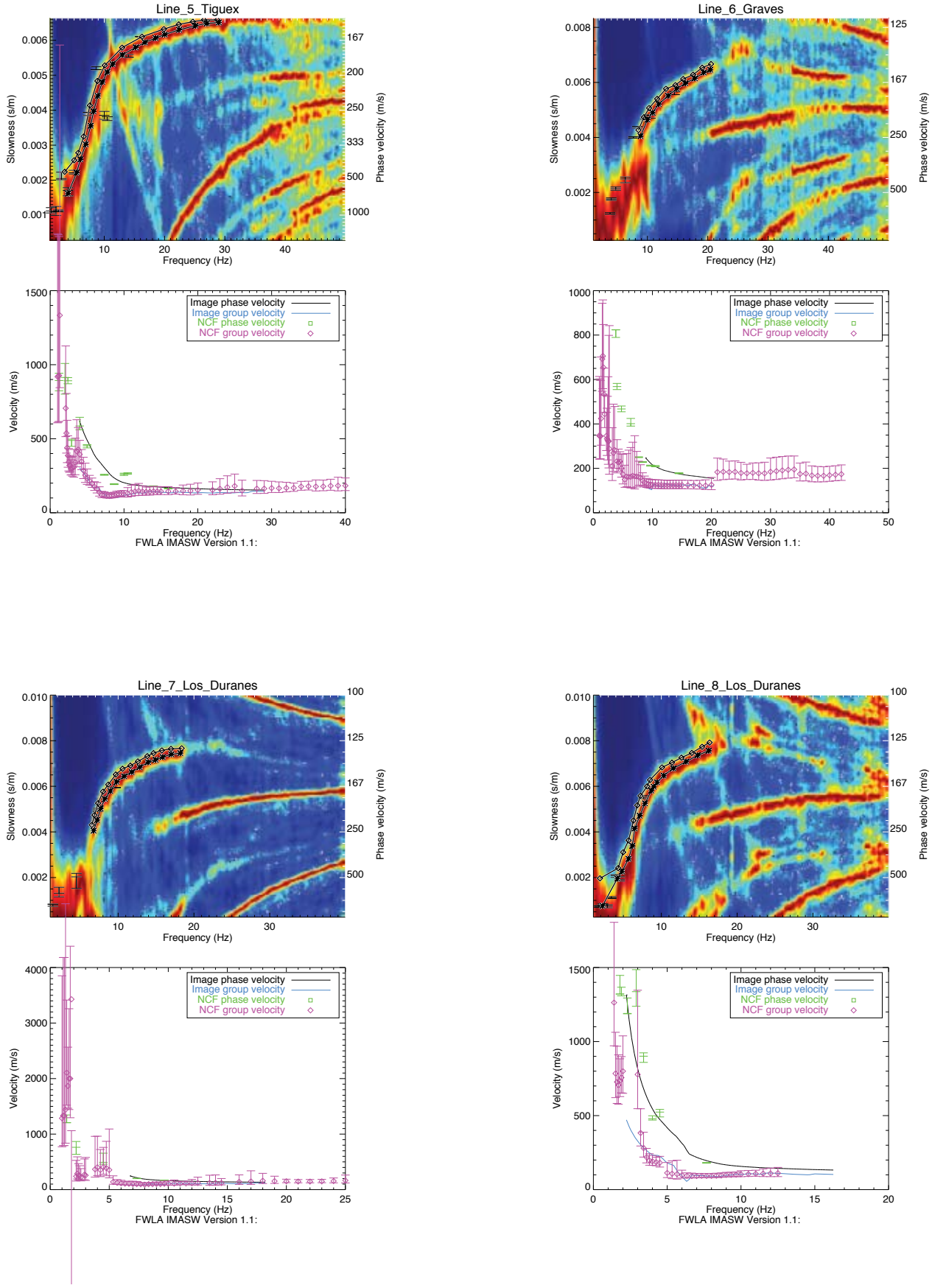

Figure B-2. Rayleigh-wave dispersion images with phase- and group-velocity picks

GRAPHICS, Projects 2068, ABQ NEHRP, modified 11.23.10

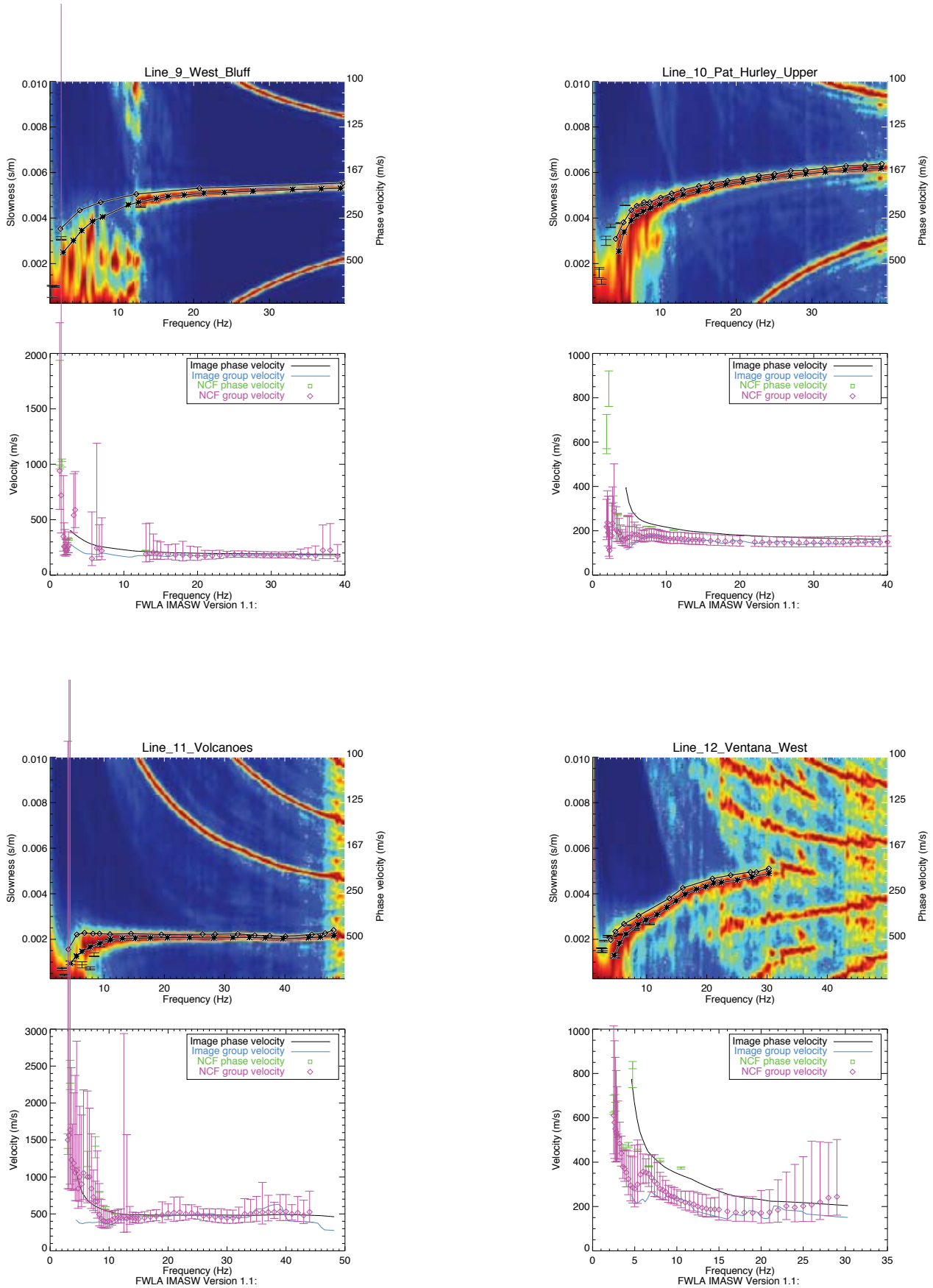

Figure B-3. Rayleigh-wave dispersion images with phase- and group-velocity picks

GRAPHICS, Projects 2068, ABQ NEHRP, modified 11.23.10

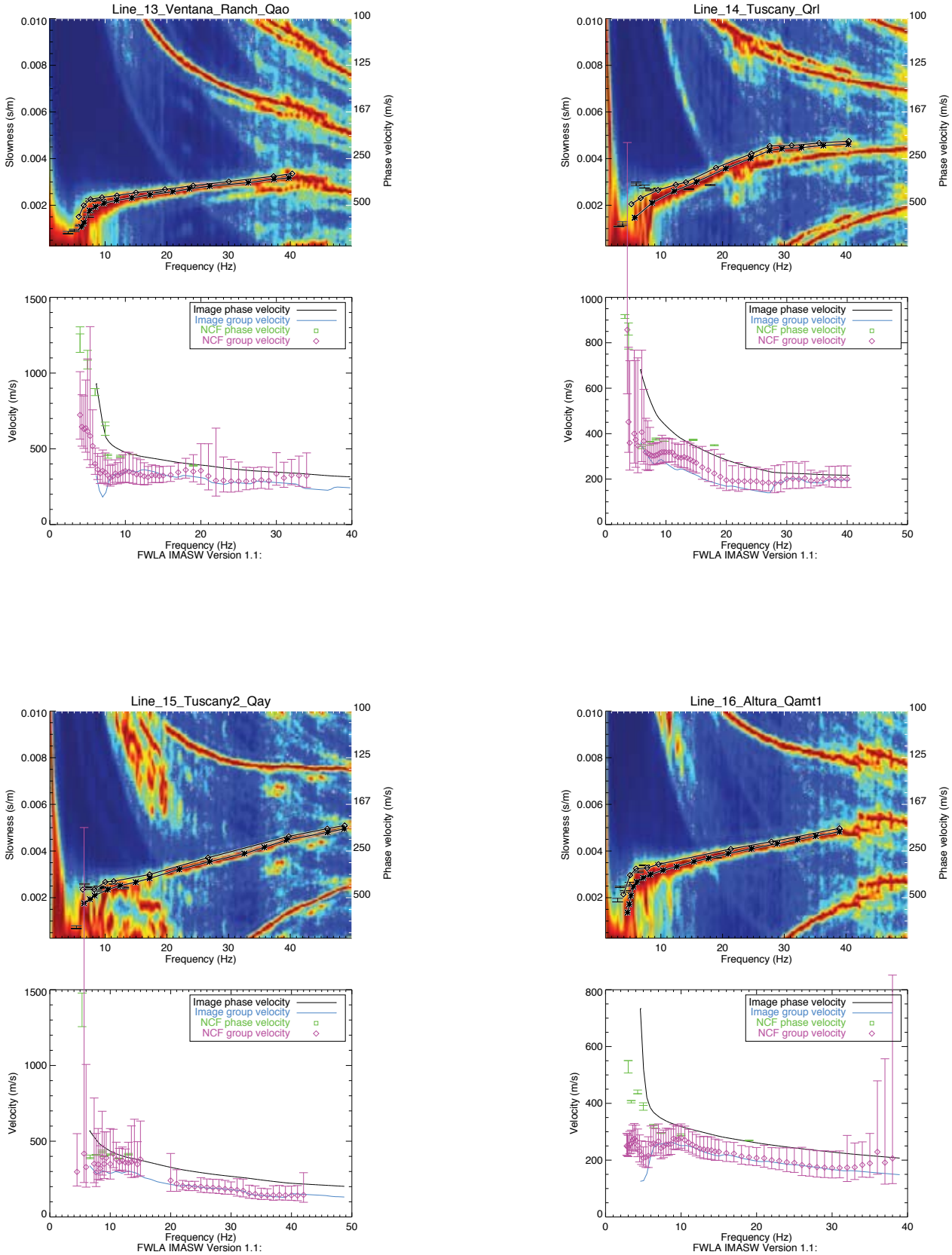

Figure B-4. Rayleigh-wave dispersion images with phase- and group-velocity picks

GRAPHICS, Projects 2068, ABQ NEHRP, modified 11.23.10

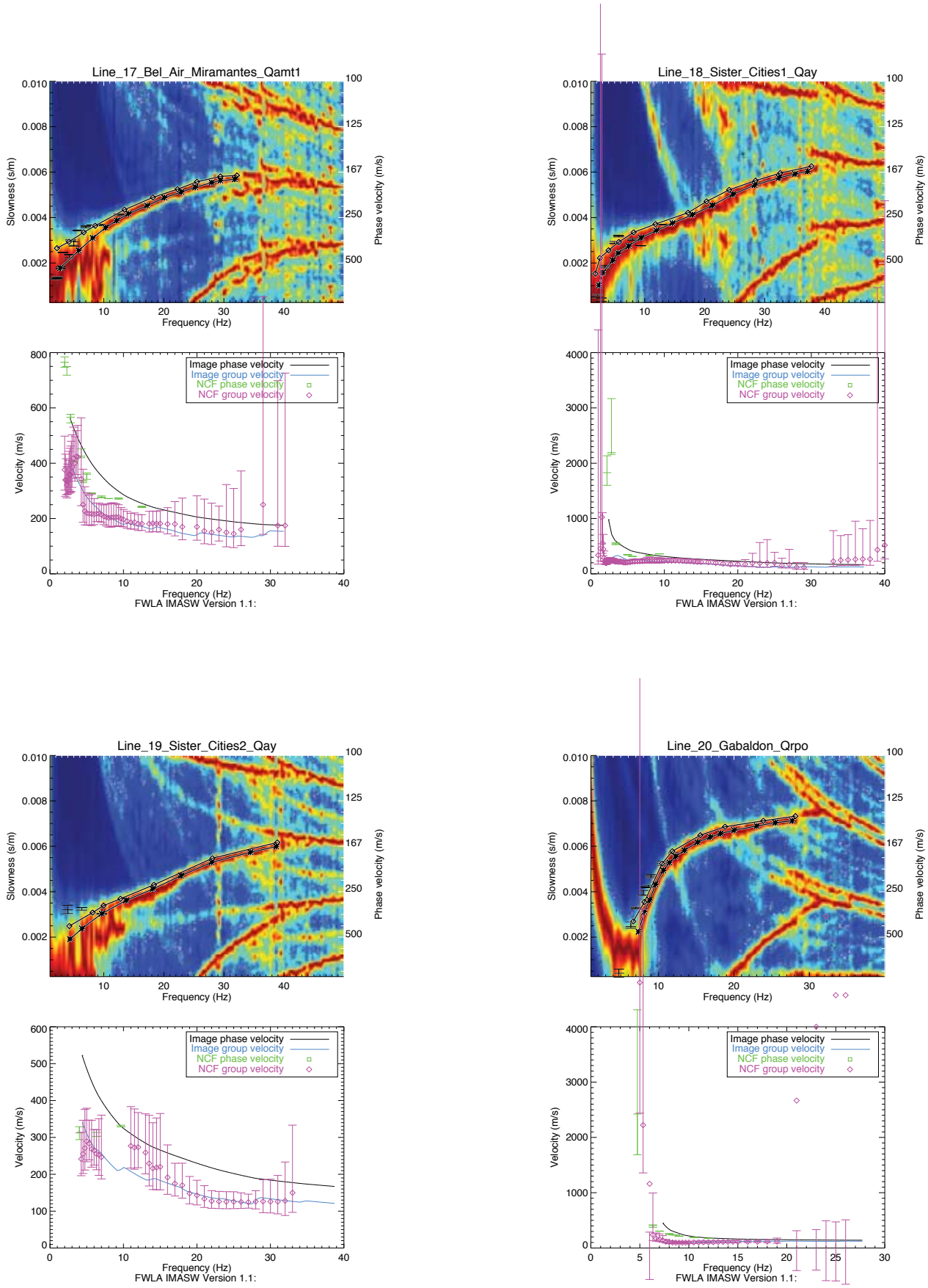

GRAPHICS, Projects 2068, ABQ NEHRP, modified 11.23.10

Figure B-5. Rayleigh-wave dispersion images with phase- and group-velocity picks

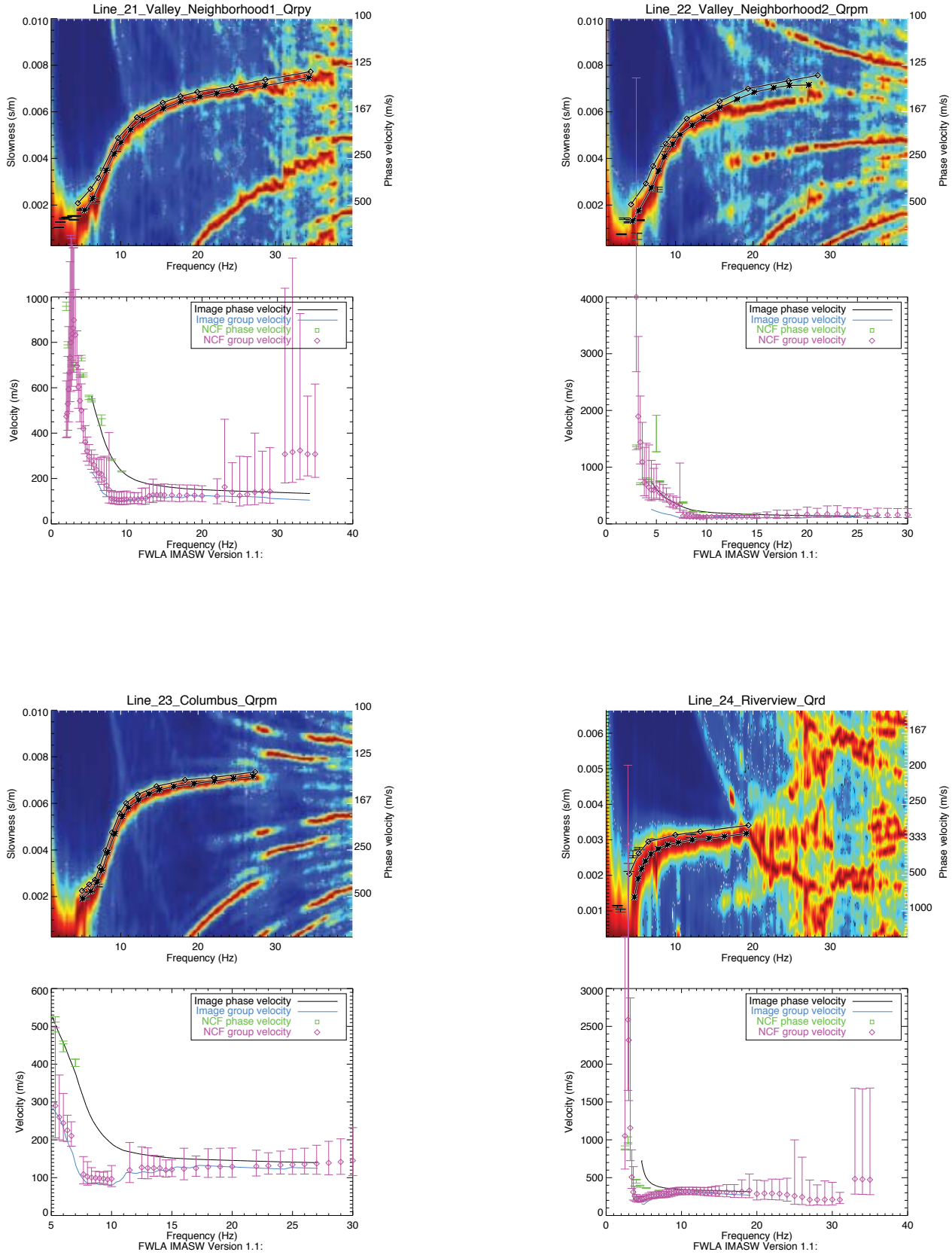

Figure B-6. Rayleigh-wave dispersion images with phase- and group-velocity picks

GRAPHICS, Projects 2068, ABQ NEHRP, modified 11.23.10

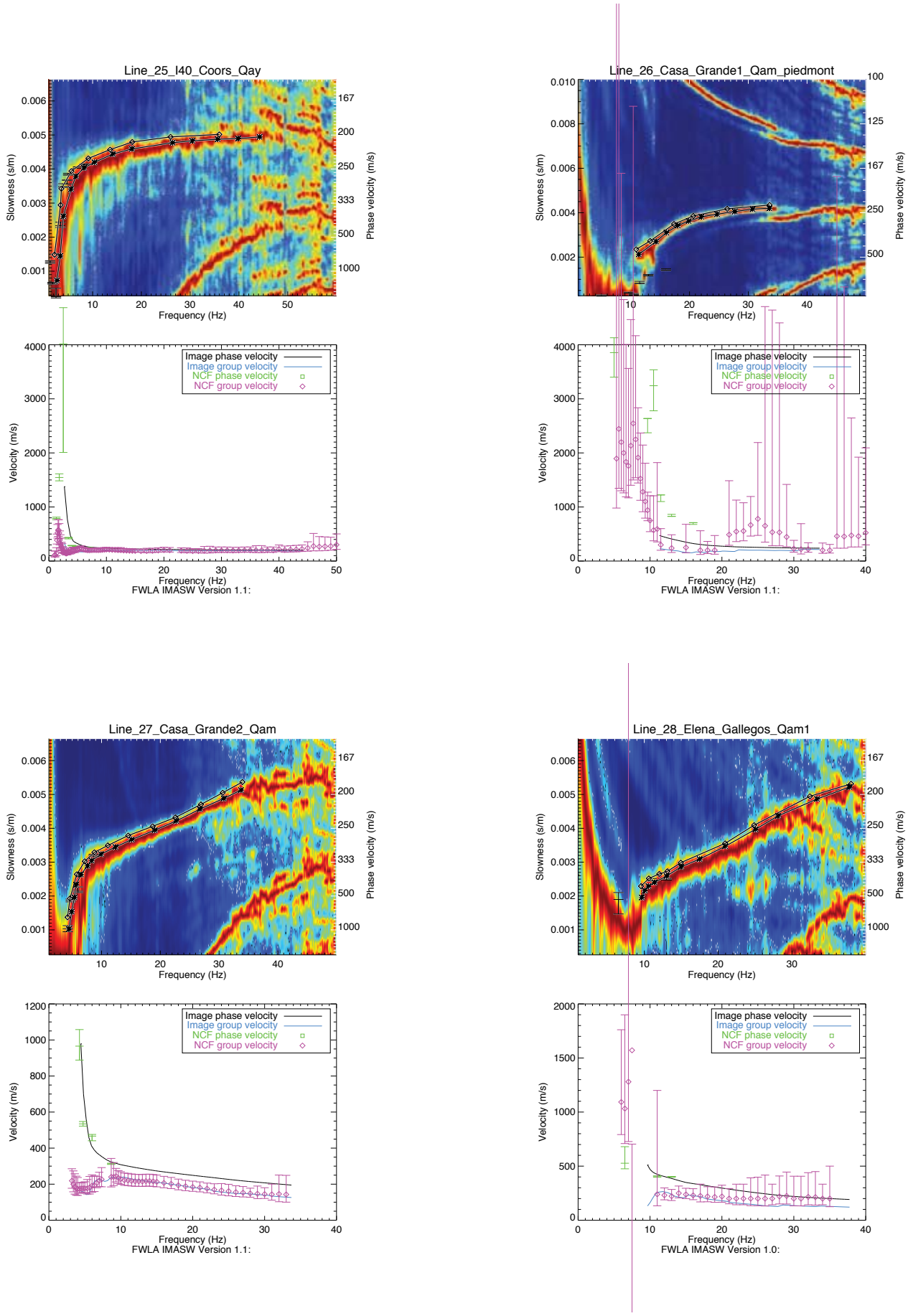

Figure B-7. Rayleigh-wave dispersion images with phase- and group-velocity picks

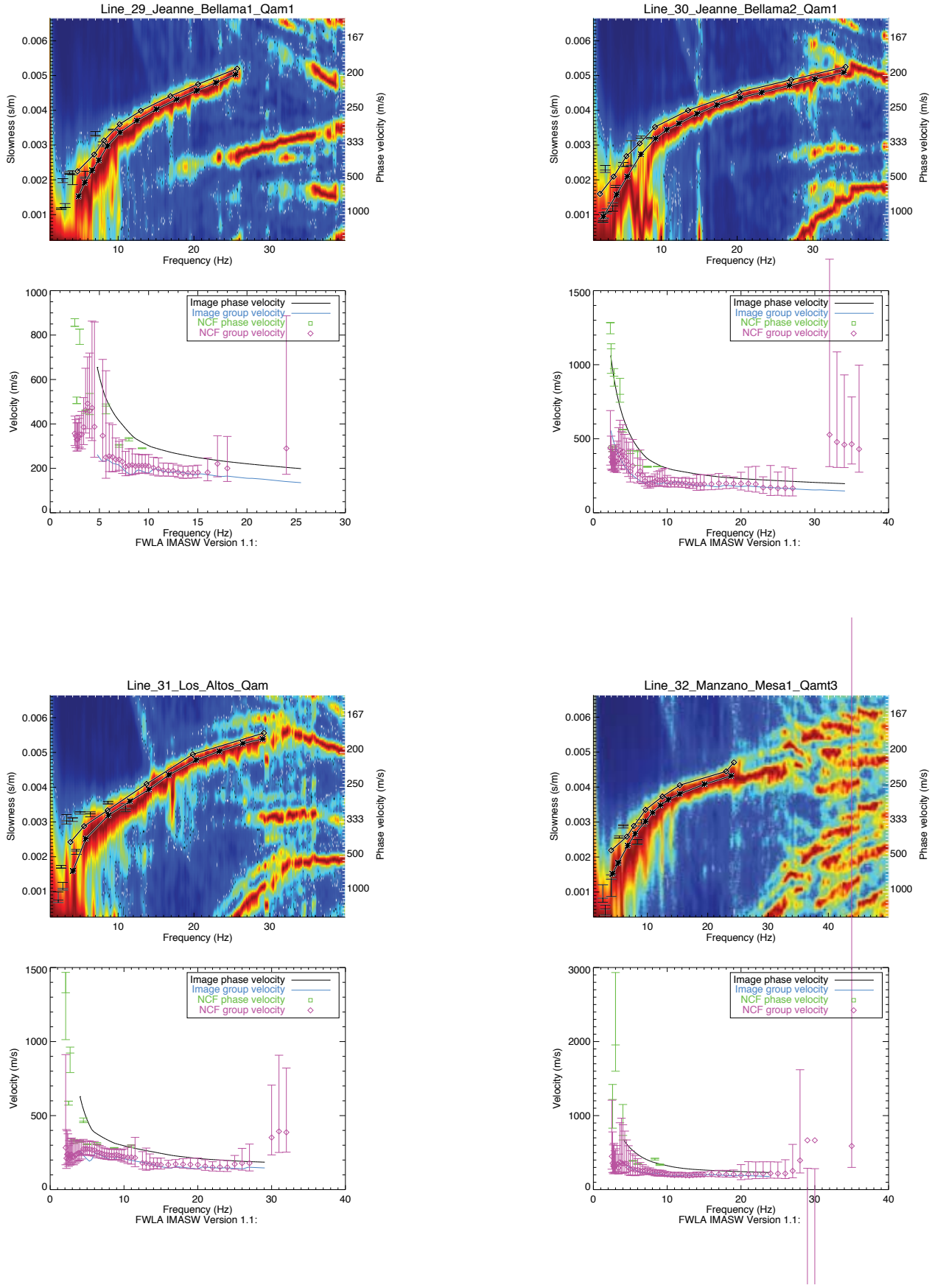

Figure B-8. Rayleigh-wave dispersion images with phase- and group-velocity picks

GRAPHICS, Projects 2068, ABQ NEHRP, modified 11.23.10

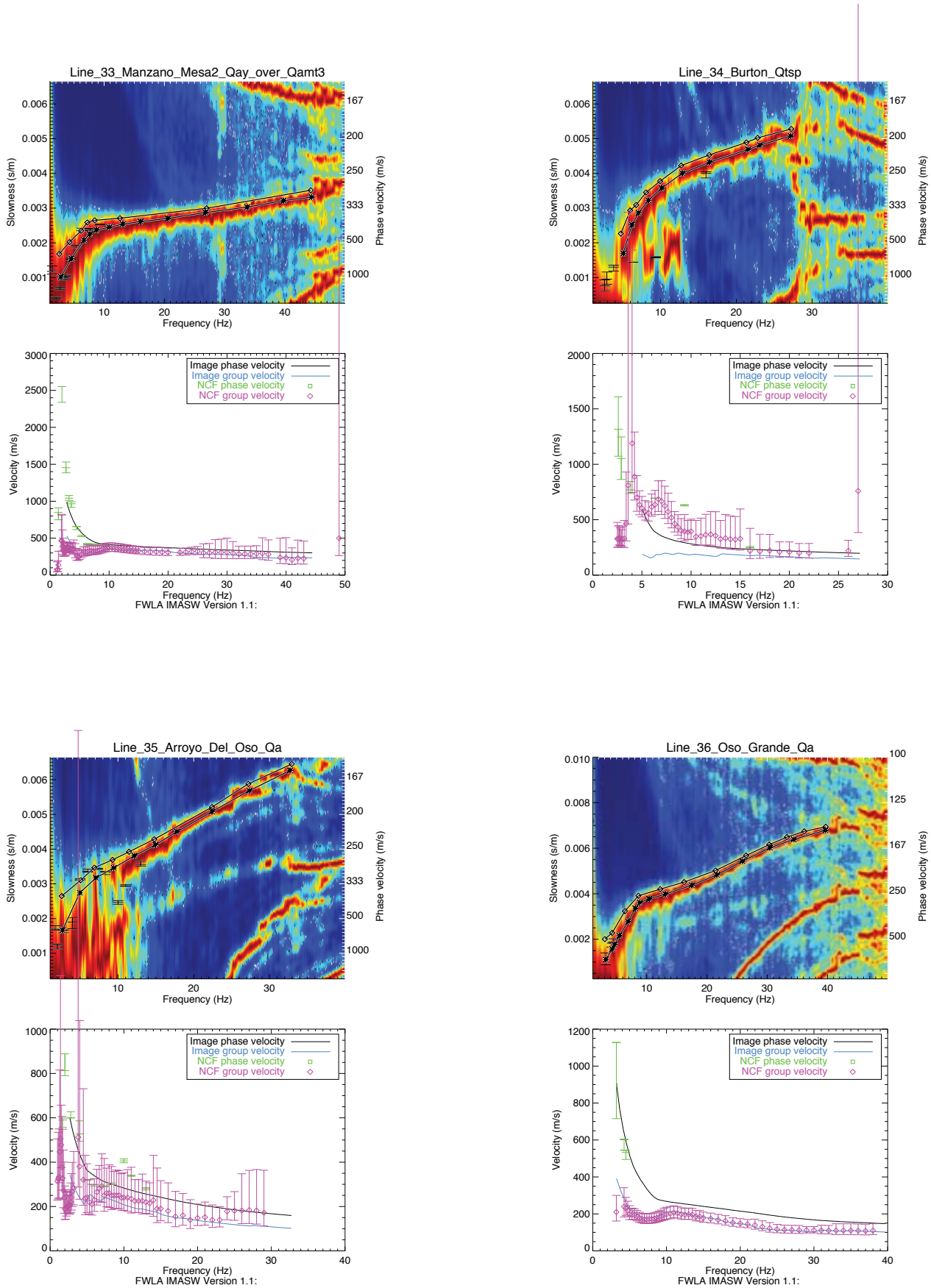

Figure B-9. Rayleigh-wave dispersion images with phase- and group-velocity picks

GRAPHICS, Projects 2068, ABQ NEHRP, modified 11.23.10

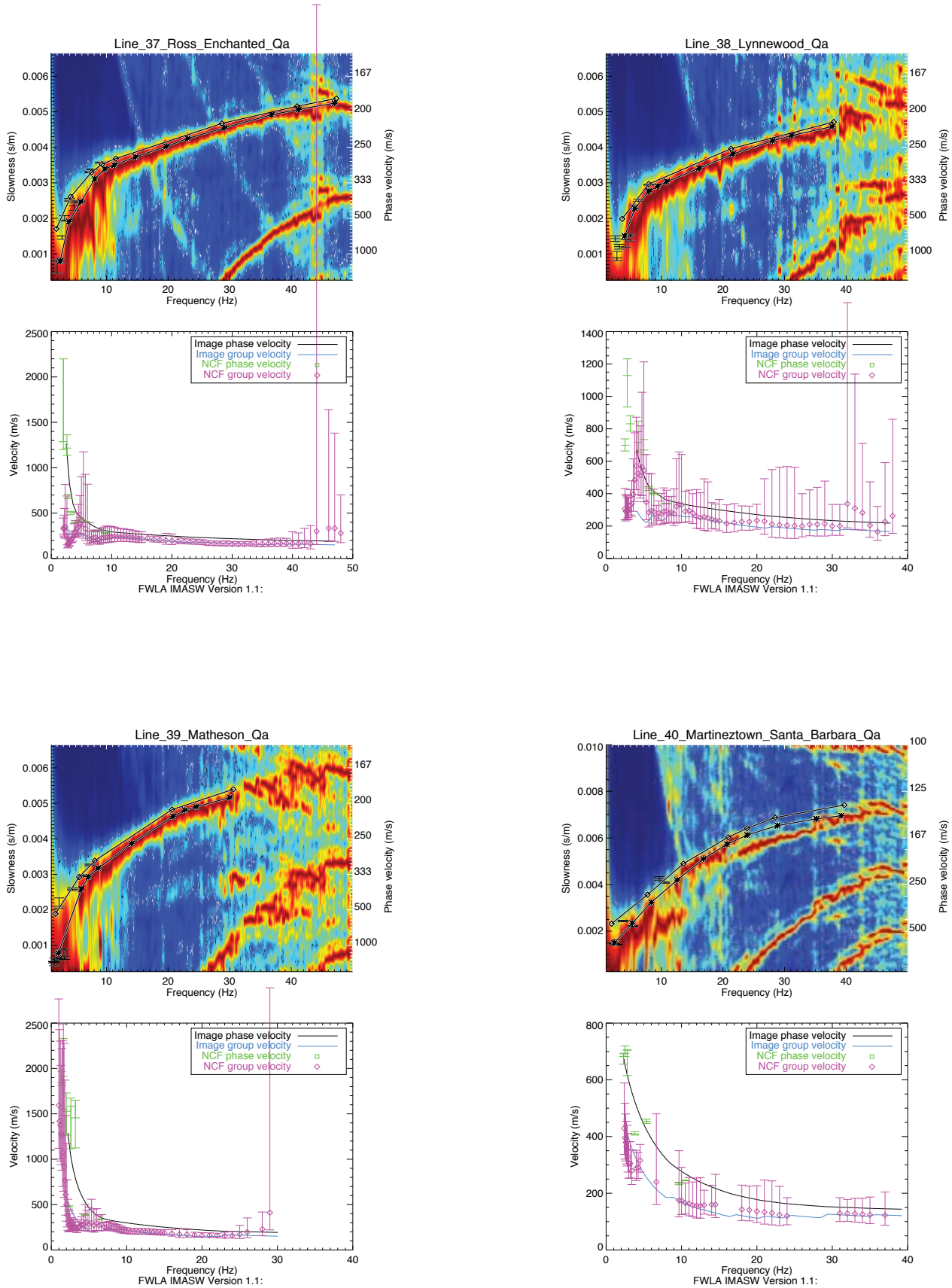

Figure B-10. Rayleigh-wave dispersion images with phase- and group-velocity picks

GRAPHICS, Projects 2068, ABQ NEHRP, modified 11.23.10

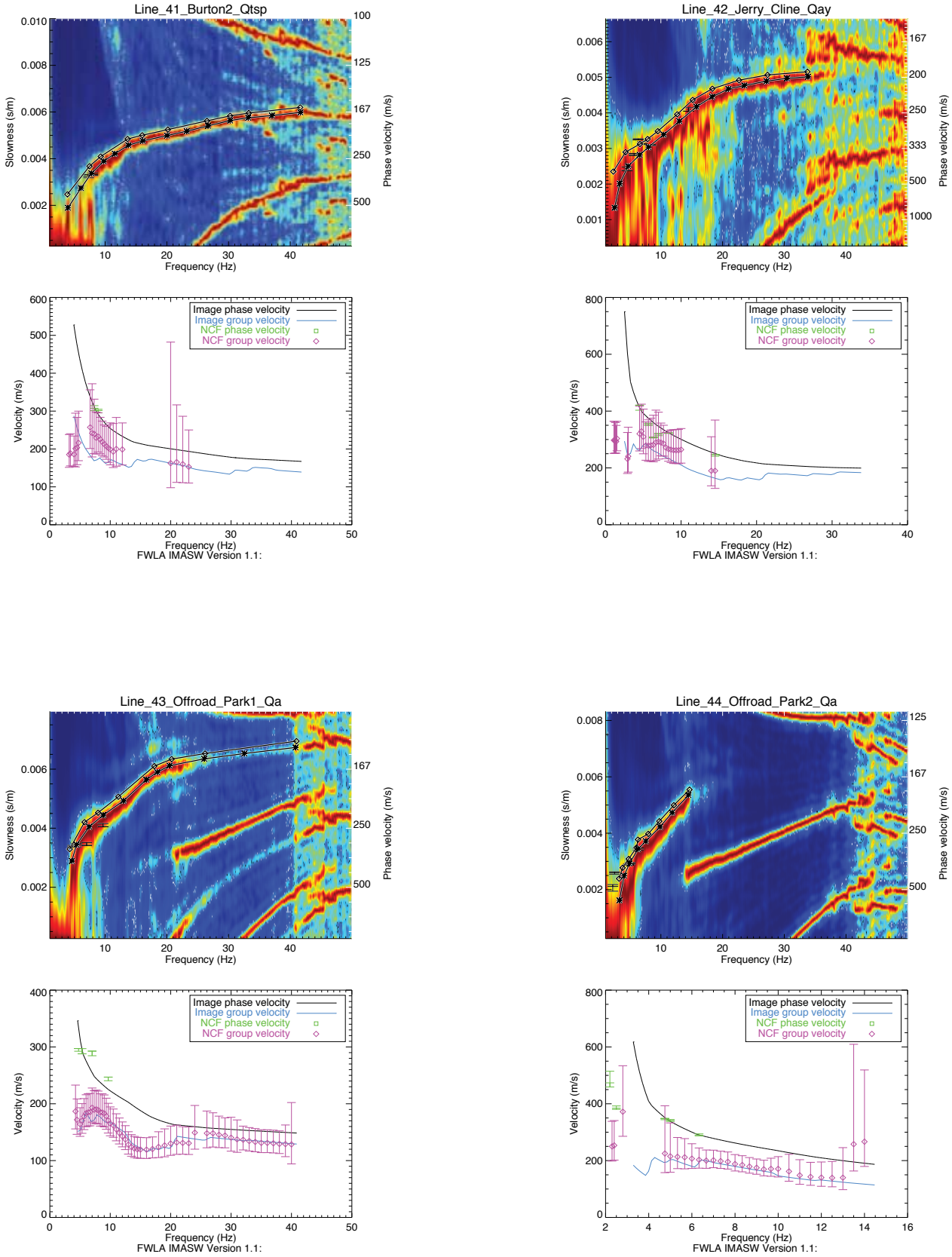

Figure B-11. Rayleigh-wave dispersion images with phase- and group-velocity picks

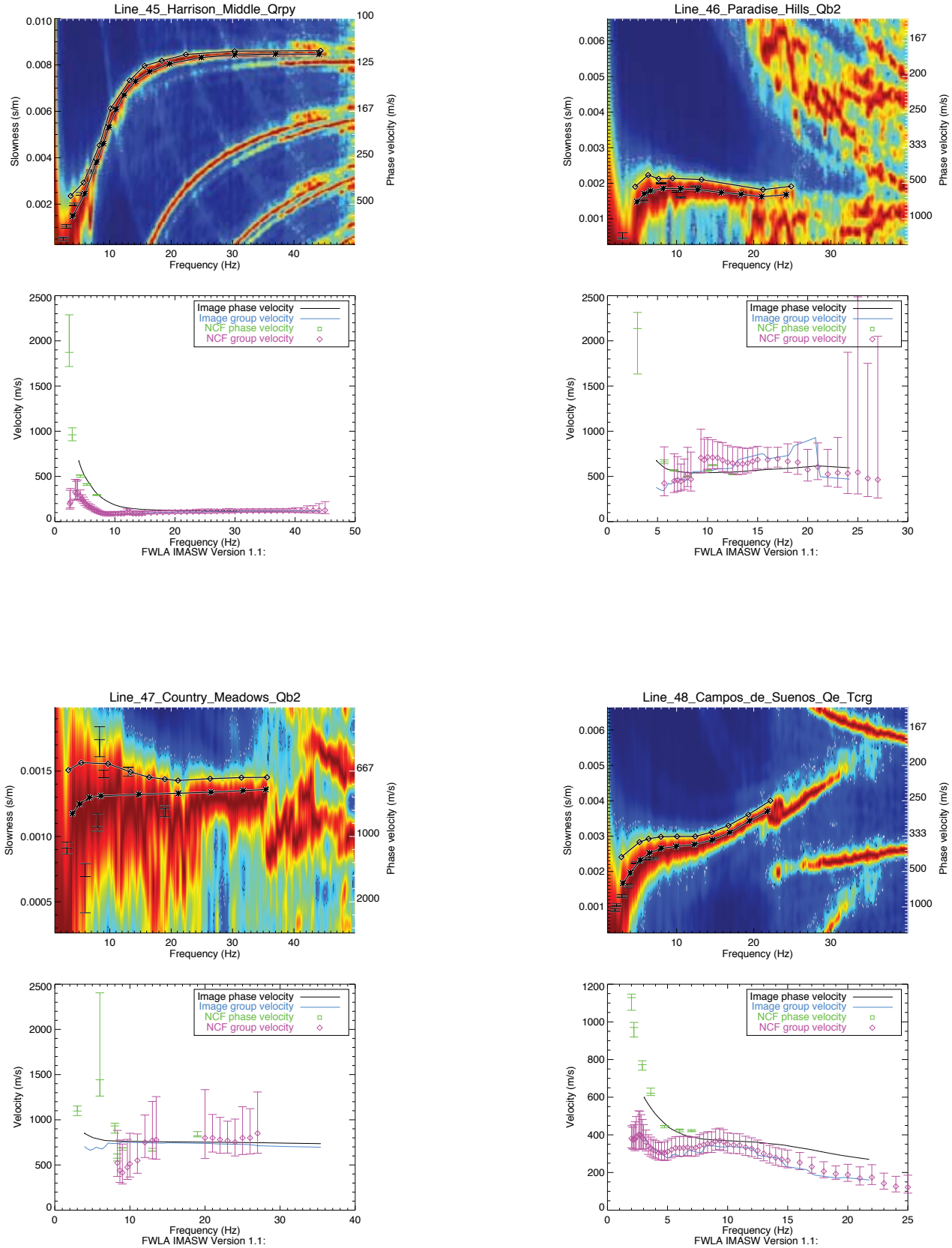

Figure B-12. Rayleigh-wave dispersion images with phase- and group-velocity picks

GRAPHICS, Projects 2068, ABQ NEHRP, modified 11.23.10

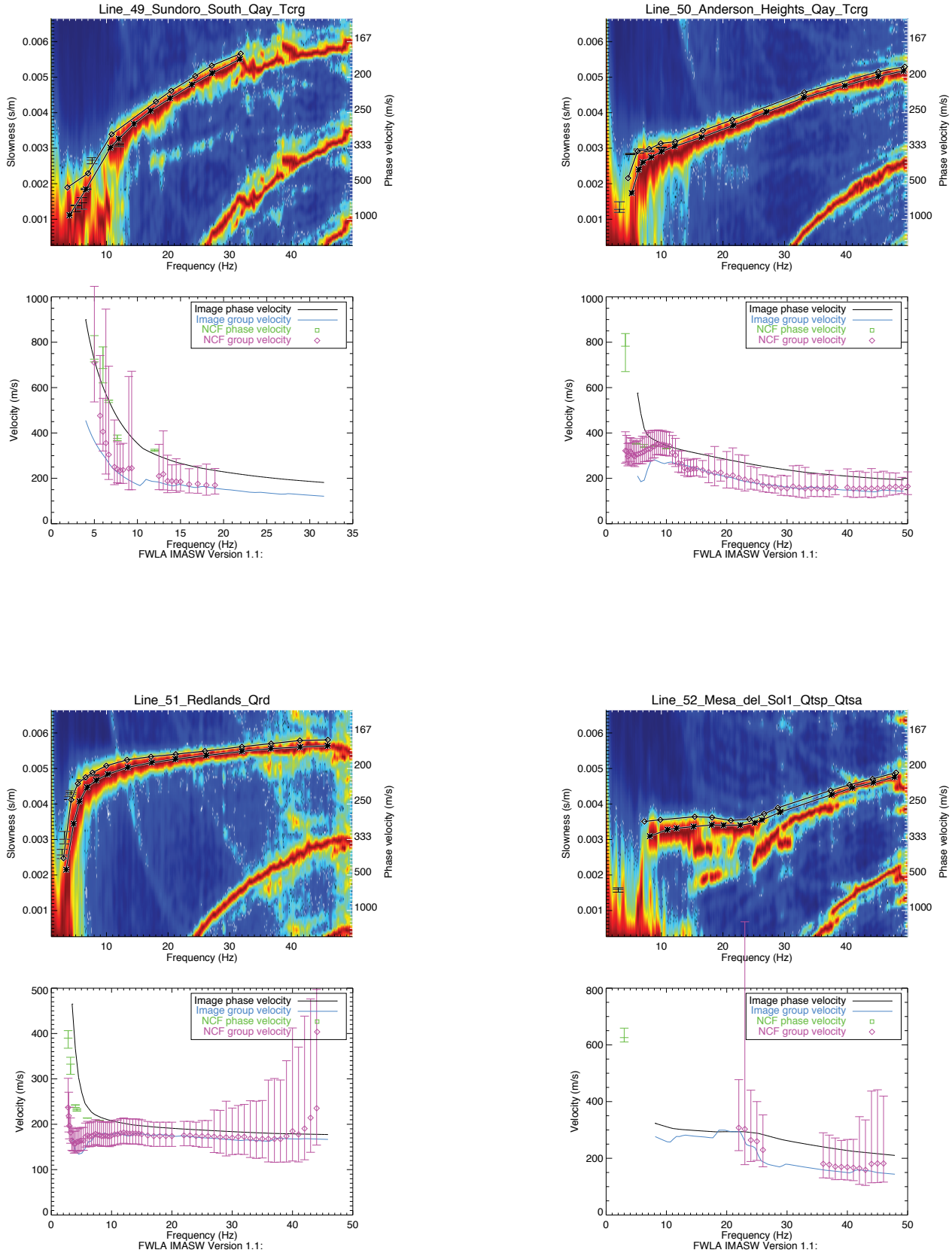

Figure B-13. Rayleigh-wave dispersion images with phase- and group-velocity picks

GRAPHICS, Projects 2068, ABQ NEHRP, modified 11.23.10

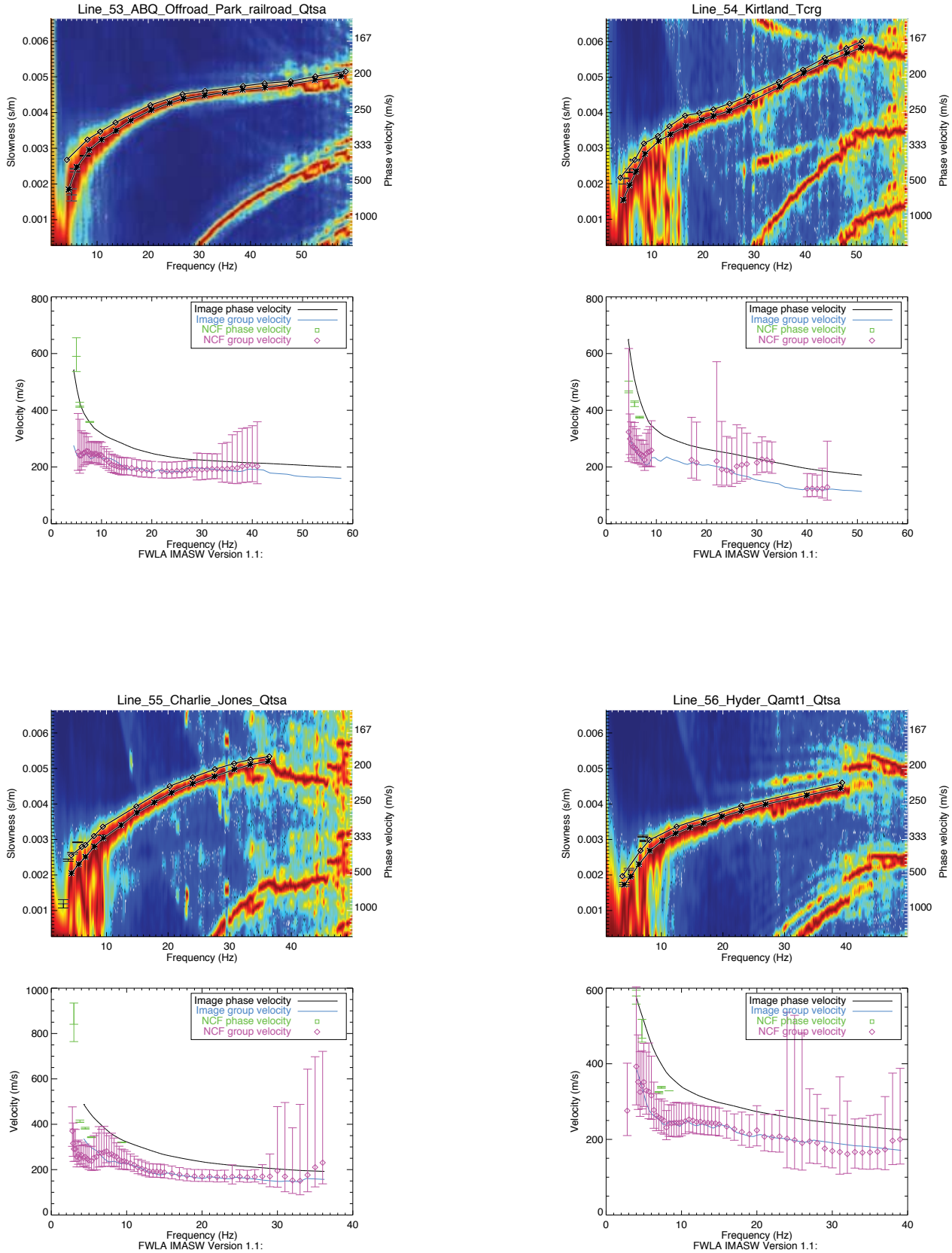

GRAPHICS, Projects 2068, ABQ NEHRP, modified 11.23.10

Figure B-14. Rayleigh-wave dispersion images with phase- and group-velocity picks

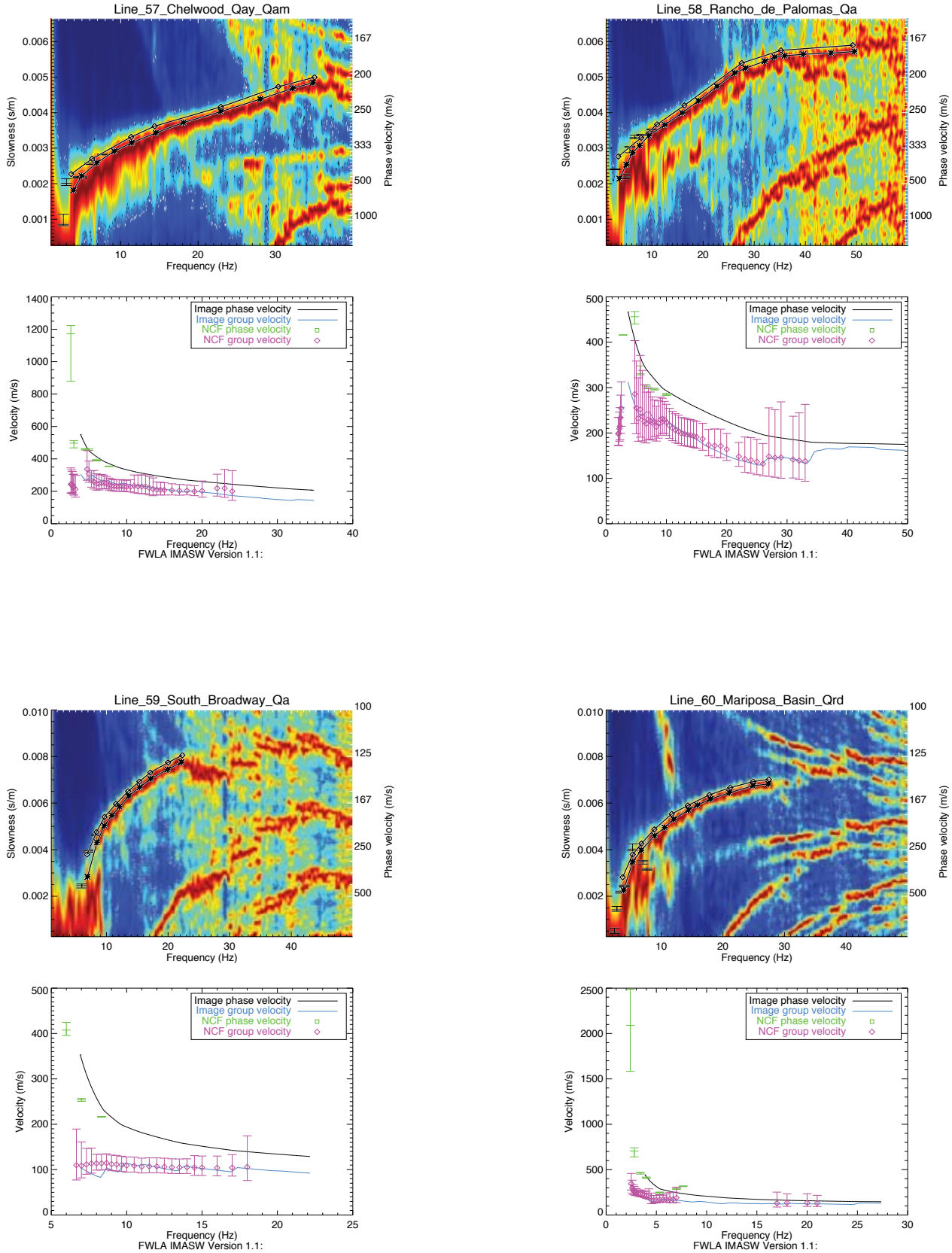

Figure B-15. Rayleigh-wave dispersion images with phase- and group-velocity picks

GRAPHICS, Projects 2068, ABQ NEHRP, modified 11.23.10

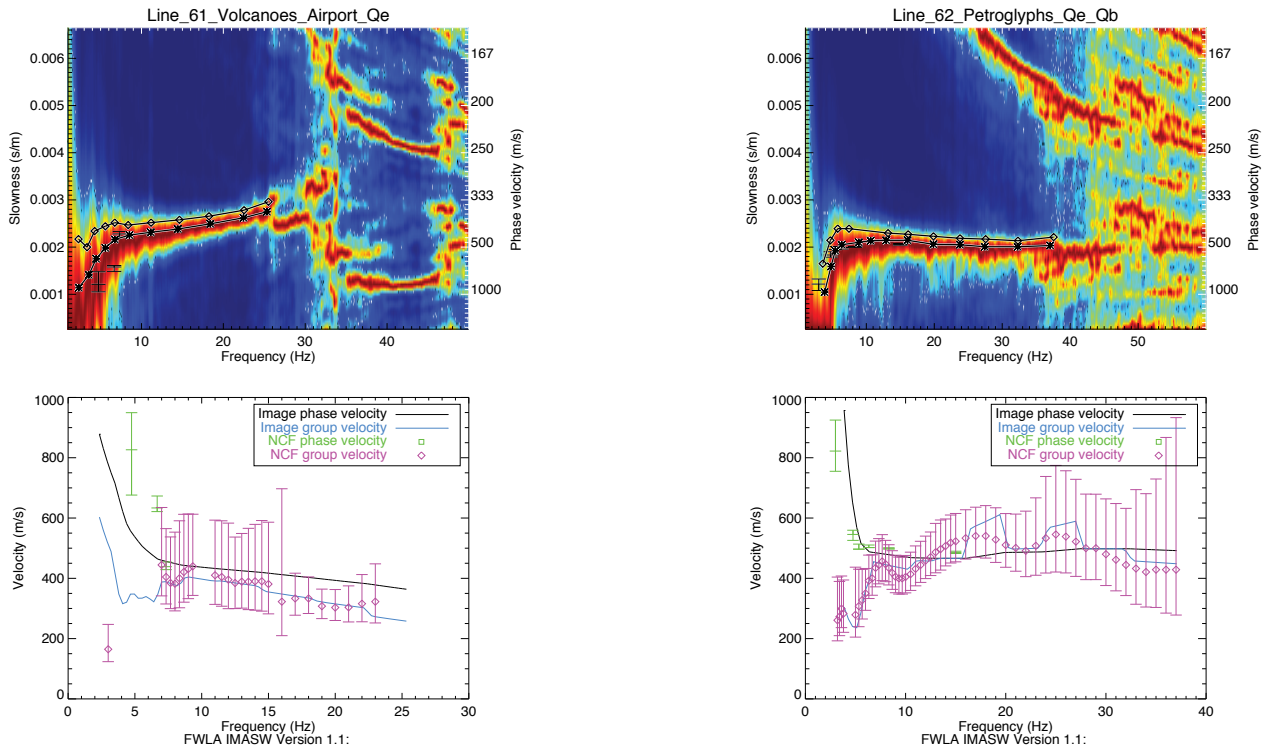

GRAPHICS, Projects 2068, ABQ NEHRP, modified 11.23.10

Figure B-16. Rayleigh-wave dispersion images with phase- and group-velocity picks